

Test-field method for mean-field coefficients with MHD background

M. Rheinhardt¹ and A. Brandenburg^{1,2}

¹ NORDITA, AlbaNova University Center, Roslagstullsbacken 23, SE-10691 Stockholm, Sweden

² Department of Astronomy, AlbaNova University Center, Stockholm University, SE-10691 Stockholm, Sweden

November 5, 2018, Revision: 1.154

ABSTRACT

Aims. The test-field method for computing turbulent transport coefficients from simulations of hydromagnetic flows is extended to the regime with a magnetohydrodynamic (MHD) background.

Methods. A generalized set of test equations is derived using both the induction equation and a modified momentum equation. By employing an additional set of auxiliary equations, we derive linear equations describing the response of the system to a set of prescribed test fields. Purely magnetic and MHD backgrounds are emulated by applying an electromotive force in the induction equation analogously to the ponderomotive force in the momentum equation. Both forces are chosen to have Roberts flow-like geometry.

Results. Examples with an MHD background are studied where the previously used quasi-kinematic test-field method breaks down. In cases with homogeneous mean fields it is shown that the generalized test-field method produces the same results as the imposed-field method, where the field-aligned component of the actual electromotive force from the simulation is used. Furthermore, results for the turbulent diffusivity tensor are given, which are inaccessible to the imposed-field method. For MHD backgrounds, new mean-field effects are found that depend on the occurrence of cross-correlations between magnetic and velocity fluctuations. For strong imposed fields, α is found to be quenched proportional to the fourth power of the field strength, regardless of the type of background studied.

Key words. magnetohydrodynamics (MHD) – turbulence – Sun: magnetic fields – stars: magnetic fields

1. Introduction

Astrophysical bodies such as stars with outer convective envelopes, accretion discs, and galaxies tend to be magnetized. In all those cases the magnetic field varies on a broad spectrum of scales. On small scales the magnetic field might well be the result of scrambling an existing large-scale field by a small-scale flow. However, at large magnetic Reynolds numbers, i.e. when advection dominates over magnetic diffusion, another source of small-scale fields is small-scale dynamo action (Kazantsev 1968). This process is now fairly well understood and confirmed by numerous simulations (Cho & Vishniac 2000; Schekochihin et al. 2002, 2004; Haugen et al. 2003, 2004); for a review see Brandenburg & Subramanian (2005). Especially in the context of magnetic fields of galaxies, the occurrence of small-scale dynamos may be important for providing a strong field on short time scales (10^7 yr), which may then act as a seed for the large-scale dynamo (Beck et al. 1994).

In contemporary galaxies the magnetic fields on small and large length scales are comparable (Beck et al. 1996), but in stars this is less clear. On the solar surface the solar magnetic field shows significant amounts of small-scale fields (Solanki et al. 2006). The possibility of generating such magnetic fields locally in the upper layers of the convection zone by a small-scale dynamo is sometimes referred to as surface dynamo (Cattaneo 1999; Emonet & Cattaneo 2001; Vögler & Schüssler 2007). On the other hand, simulations of stratified convection with shear show that small-scale dynamo action is a prevalent feature of the kinematic

regime, but becomes less important when the field is strong and has saturated (Brandenburg 2005a; Käpylä et al. 2008).

An important question is then how the primary presence of small-scale magnetic fields affects the generation of large-scale fields if these are the result of a dynamo process that produces magnetic fields on scales large compared with those of the energy-carrying eddies of the underlying and in general turbulent flow (Parker 1979) via an instability. A commonly used tool for studying these large-scale dynamos is mean-field electrodynamics, where correlations of small-scale magnetic and velocity fields are expressed in terms of the mean magnetic field and the mean velocity using corresponding turbulent transport coefficients or their associated integral kernels (Moffatt 1978; Krause & Rädler 1980). The determination of these coefficients (e.g., α effect and turbulent diffusivity) is the central task of mean-field dynamo theory. This can be performed analytically, but usually only via approximations which are hardly justified in realistic astrophysical situations where the magnetic Reynolds numbers, Re_M , are large.

Obtaining turbulent transport coefficients from direct numerical simulations (DNS) offers a more sustainable alternative as it avoids the restricting approximations and uncertainties of analytic approaches. Moreover, no assumptions concerning correlation properties of the turbulence need to be made, because a direct “measurement” of those properties is performed in a physically consistent situation emulated by the DNS. The simplest way to accomplish such a measurement is to include, in the DNS, an imposed large-scale (typically uniform) magnetic field whose influence on the fluctuations of magnetic field and velocity is utilized to

infer some of the full set of transport coefficients. We refer to this technique as the *imposed-field method*.

A more universal tool is offered by the test-field method (Schrinner et al. 2005, 2007), which allows the determination of all wanted transport coefficients from a single DNS. For this purpose the fluctuating velocity is taken from the DNS and inserted into a properly tailored set of *test equations*. Their solutions, the *test solutions* represent fluctuating magnetic fields as responses to the interaction of the fluctuating velocity with a set of properly chosen mean fields. These mean fields will be called *test fields*. For distinction from the test equations, which are in general also solved by direct numerical simulation, we will refer to the original DNS as the *main run*. This method has been successfully applied to homogeneous turbulence with helicity (Sur et al. 2008, Brandenburg et al. 2008a), with shear and no helicity (Brandenburg et al. 2008b), and with both (Mitra et al. 2009).

A crucial requirement on any test-field method is the independence of the resulting transport coefficients on the strength and geometry of the test fields. This is immediately clear in the kinematic situation, i.e., if there is no back-reaction of the mean magnetic field on the flow. Indeed, for given magnetic boundary conditions and a given value for the magnetic diffusivity, the transport coefficients must not reflect anything else than correlation properties of the velocity field which are completely determined by the hydrodynamics alone. For this to be guaranteed the test equations have to be linear and the test solutions have to be linear and homogeneous in the test fields.

Beyond the kinematic situation the same requirement still holds, although the flow is now modified by a mean magnetic field occurring in the main run. (Whether it is maintained by external sources or generated by a dynamo process does not matter in this context.) Consequently, the transport coefficients are now functions of this mean field. It is no longer so obvious that under these circumstances a test-field method with the aforementioned linearity and homogeneity properties can be established at all. Nevertheless, it turned out that the test-field method developed for the kinematic situation gives consistent results even in the nonlinear case without any modification (Brandenburg et al. 2008c). This method, which we will refer to as “quasi-kinematic” is, however, restricted to situations in which the magnetic fluctuations are solely a consequence of the mean magnetic field. (That is, the primary or background turbulence is purely hydrodynamic.)

The power of the quasi-kinematic method was demonstrated based on a simulation of an α^2 dynamo where the main run has reached saturation with mean magnetic fields being Beltrami fields (Brandenburg et al. 2008c). Magnetic and fluid Reynolds numbers up to 600 were taken into account, so in some of the high Re_M runs there was certainly small-scale dynamo action, that is, a primary magnetic turbulence \mathbf{b}_0 should be expected. Nevertheless, the quasi-kinematic method was found to work reliably even for strongly saturated dynamo fields. This was revealed by verifying that the analytically solvable mean-field dynamo model employing the values of α and turbulent diffusivity as derived from the saturated state of the main run indeed yielded a vanishing growth rate. Very likely the small-scale dynamo had saturated on a low level so the contribution to the mean electromotive force, which was not taken into

account by the quasi-kinematic method, could not create a marked error.

Limitations of the quasi-kinematic test-field method were recently pointed out by Courvoisier et al. (2010) and will be commented upon in more detail in the discussion section. Indeed, the purpose of our work is to propose a generalized test-field method that allows for the presence of magnetic fluctuations in the background turbulence. Moreover, its validity range should cover dynamically effective mean fields, that is, situations in which the velocity and magnetic field fluctuations are significantly affected by the mean field.

With a view to this generalization we will first recall the mathematical justification of the quasi-kinematic method and indicate the reason for its limited applicability (Sect. 2). In Sect. 3 the foundation of the generalized method will be laid down in the context of a relevant set of model equations. In Sect. 4 results will be presented for various combinations of hydrodynamic and magnetic backgrounds having Roberts-flow geometry. The astrophysical relevance of our results and the connection with the work of Courvoisier et al. (2010) will be discussed in Sect. 5.

2. Justification of the quasi-kinematic test-field method and its limitation

In the following we split any relevant physical quantity F into mean and fluctuating parts, \bar{F} and f . No specific averaging procedure will be adopted at this point; we merely assume the Reynolds rules to be obeyed. Furthermore, we split the fluctuations of magnetic field and velocity, \mathbf{b} and \mathbf{u} , into parts existing already in the absence of a mean magnetic field, \mathbf{b}_0 and \mathbf{u}_0 (together they form the background turbulence), and parts vanishing with $\bar{\mathbf{B}}$, denoted by $\mathbf{b}_{\bar{\mathbf{B}}}$ and $\mathbf{u}_{\bar{\mathbf{B}}}$. We may split the mean electromotive force $\bar{\mathcal{E}} = \overline{\mathbf{u} \times \mathbf{b}}$ likewise and get

$$\bar{\mathcal{E}} = \bar{\mathcal{E}}_0 + \bar{\mathcal{E}}_{\bar{\mathbf{B}}} \quad (1)$$

with

$$\bar{\mathcal{E}}_0 = \overline{\mathbf{u}_0 \times \mathbf{b}_0}, \quad (2)$$

$$\bar{\mathcal{E}}_{\bar{\mathbf{B}}} = \overline{\mathbf{u}_0 \times \mathbf{b}_{\bar{\mathbf{B}}}} + \overline{\mathbf{u}_{\bar{\mathbf{B}}} \times \mathbf{b}_0} + \overline{\mathbf{u}_{\bar{\mathbf{B}}} \times \mathbf{b}_{\bar{\mathbf{B}}}}. \quad (3)$$

Note that we do not restrict $\mathbf{b}_{\bar{\mathbf{B}}}$ and $\mathbf{u}_{\bar{\mathbf{B}}}$, and hence also not $\bar{\mathcal{E}}_{\bar{\mathbf{B}}}$ to a certain order in $\bar{\mathbf{B}}$.

In the present Section we assume that the background turbulence is purely hydrodynamic, that is, $\mathbf{b}_0 = \mathbf{0}$ and hence $\mathbf{b} = \mathbf{b}_{\bar{\mathbf{B}}}$ or, in other words, the magnetic fluctuations \mathbf{b} are entirely a consequence of the interaction of the velocity fluctuations \mathbf{u} with the mean field $\bar{\mathbf{B}}$.

In a homogeneous medium, the induction equations for the total and mean magnetic fields as well as for the magnetic fluctuations read

$$\frac{\partial \mathbf{B}}{\partial t} = \eta \nabla^2 \mathbf{B} + \text{curl}(\mathbf{U} \times \mathbf{B}), \quad (4)$$

$$\frac{\partial \bar{\mathbf{B}}}{\partial t} = \eta \nabla^2 \bar{\mathbf{B}} + \text{curl}(\bar{\mathbf{U}} \times \bar{\mathbf{B}} + \bar{\mathcal{E}}), \quad (5)$$

$$\frac{\partial \mathbf{b}}{\partial t} = \eta \nabla^2 \mathbf{b} + \text{curl}(\bar{\mathbf{U}} \times \mathbf{b} + \mathbf{u} \times \bar{\mathbf{B}} + \mathcal{E}'), \quad (6)$$

with $\mathcal{E}' = \mathbf{u} \times \mathbf{b} - \overline{\mathbf{u} \times \mathbf{b}}$. The solution of the linear equation (6) for the fluctuations \mathbf{b} , considered as a functional of \mathbf{u} ,

$\overline{\mathbf{U}}$ and $\overline{\mathbf{B}}$, is linear and homogeneous in the latter and the same is true for

$$\overline{\mathcal{E}}_{\overline{\mathbf{B}}} = \overline{\mathcal{E}} = \overline{\mathbf{u} \times \mathbf{b}_{\overline{\mathbf{B}}}} = \overline{\mathbf{u}} \times \overline{\mathbf{b}}. \quad (7)$$

If the velocity is influenced by the mean field, that is, if \mathbf{u} and $\overline{\mathbf{U}}$ depend on $\overline{\mathbf{B}}$, $\overline{\mathcal{E}}$ considered as a functional of $\overline{\mathbf{B}}$, $\overline{\mathcal{E}}\{\overline{\mathbf{B}}\}$, is of course nonlinear. However, $\overline{\mathcal{E}}$, again considered as a functional of \mathbf{u} , $\overline{\mathbf{U}}$ and $\overline{\mathbf{B}}$, $\overline{\mathcal{E}}\{\mathbf{u}, \overline{\mathbf{U}}, \overline{\mathbf{B}}\}$, is still linear in $\overline{\mathbf{B}}$.

The major task of mean-field theory consists now just in establishing a linear and homogeneous functional relating $\overline{\mathcal{E}}$ and $\overline{\mathbf{B}}$. Making the ansatz

$$\overline{\mathcal{E}} = \alpha \overline{\mathbf{B}} - \eta \nabla \overline{\mathbf{B}}, \quad (8)$$

with $\nabla \overline{\mathbf{B}}$ being the gradient tensor of the mean magnetic field, this task coincides with determining the tensors α and η , which are of course functionals of \mathbf{u} and $\overline{\mathbf{U}}$. Because of linearity and homogeneity we are entitled to employ for this purpose various *arbitrary* vector fields $\overline{\mathbf{B}}^T$ (i.e., test fields) in place of $\overline{\mathbf{B}}$ in (6), keeping the velocity of course fixed. Each specific assignment of $\overline{\mathbf{B}}^T$ yields a corresponding \mathbf{b}^T and via that an $\overline{\mathcal{E}}^T$ and it establishes (up to) three linear equations for the wanted components of α and η . Hence, choosing the number of test fields in accordance with the number of the tensor components, and specifying the geometry of the test fields “sufficiently independent” from each other, the components of α and η can be determined uniquely. In doing so, the amplitude of the test fields clearly drops out (Brandenburg et al. 2008b).

Is the result affected by the *geometry* of the test fields? An ansatz like (8) is in general not exhaustive, but restricted in its validity to a certain class of mean fields, here strictly speaking to stationary fields which change at most linearly in space. Consequently, the geometry of the test fields is without relevance just as long as they are taken from the class for which the $\overline{\mathcal{E}}$ ansatz is valid, but not for other choices.

For many applications it will be useful to generalize the test-field method such that all employed test-fields are harmonic functions of position, defined by one and the same wavevector \mathbf{k} . The turbulent transport coefficients can then be obtained as functions of \mathbf{k} and have to be identified with the Fourier transforms of integral kernels which define the in general non-local relationship between $\overline{\mathcal{E}}$ and $\overline{\mathbf{B}}$ (Brandenburg et al. 2008a). Quite analogous, the in general also non-instantaneous relationship between these quantities can be recovered by using harmonic functions of time for the test-fields. The coefficients, then depending on the angular frequency ω , represent again Fourier transforms of the corresponding integral kernels (Hubbard & Brandenburg 2009).

If \mathbf{u} and $\overline{\mathbf{U}}$ are taken from a series of main runs with a dynamically effective mean field of, say, fixed geometry, but from run to run differing strength $\overline{\mathbf{B}}$, α and η can be obtained as functions of $\overline{\mathbf{B}}$. Thus, it is possible to determine the *quenched* dynamo coefficients basically in the same way as in the kinematic case, albeit at the cost of multiple numeric work.

Let us now relax the above assumption on the background turbulence and admit additionally a primary *magnetic* turbulence \mathbf{b}_0 . For the sake of simplicity we will not deal here with $\overline{\mathcal{E}}_0$, so let us assume that it vanishes. In the

representation (3) of $\overline{\mathcal{E}}$ we now combine the first and last terms using $\mathbf{u} = \mathbf{u}_0 + \mathbf{u}_{\overline{\mathbf{B}}}$ and obtain

$$\overline{\mathcal{E}} = \overline{\mathbf{u} \times \mathbf{b}_{\overline{\mathbf{B}}}} + \overline{\mathbf{u}_{\overline{\mathbf{B}}} \times \mathbf{b}_0}, \quad (9)$$

differing from (7) by the additional contribution, $\overline{\mathbf{u}_{\overline{\mathbf{B}}} \times \mathbf{b}_0}$. The quasi-kinematic method necessarily fails here even when modifying (6) appropriately to form an equation for $\mathbf{b}_{\overline{\mathbf{B}}}$ as only the term $\overline{\mathbf{u} \times \mathbf{b}_{\overline{\mathbf{B}}}}$ is provided. Obviously, a valid scheme must treat also $\mathbf{u}_{\overline{\mathbf{B}}}$ in a test-field manner similar to $\mathbf{b}_{\overline{\mathbf{B}}}$. The equation to be employed for $\mathbf{u}_{\overline{\mathbf{B}}}$ has of course to rely upon the momentum equation. Due to its intrinsic nonlinearity, however, a major challenge consists then in ensuring the linearity and homogeneity of the test solutions in the test fields.

3. A model problem

3.1. Motivation

We commence our study with a model problem that is simpler than the complete MHD setup, but nevertheless shares with it the same mathematical complications. We drop the advection and pressure terms and adopt for the diffusion operator simply the Laplacian (and a homogeneous medium). Thus, there is no constraint on the velocity from a continuity equation and an equation of state. However, as in the full problem, we allow the magnetic field to exert a Lorentz force on the fluid velocity. We also allow for the presence of an imposed uniform magnetic field \mathbf{B}_{imp} to enable a determination of the α effect independently from the test-field method. The magnetic field is hence represented as $\mathbf{B} = \mathbf{B}_{\text{imp}} + \nabla \times \mathbf{A}$ where \mathbf{A} is the vector potential of its non-uniform part. The resulting modified momentum equation for the velocity \mathbf{U} and the (original) induction equation read then

$$\frac{\partial \mathbf{U}}{\partial t} = \mathbf{J} \times \mathbf{B} + \mathbf{F}_K + \nu \nabla^2 \mathbf{U}, \quad (10)$$

$$\frac{\partial \mathbf{A}}{\partial t} = \mathbf{U} \times \mathbf{B} + \mathbf{F}_M + \eta \nabla^2 \mathbf{A}, \quad (11)$$

where we have included the possibility of both kinetic and magnetic forcing terms, \mathbf{F}_K and \mathbf{F}_M , respectively. (In this paper we use hydrodynamic and kinetic forcing synonymously.) We have adopted a system of units in which \mathbf{B} has the dimension of velocity namely $\mathbf{B} := \mathbf{B}/\sqrt{\mu\rho}$, $\rho = \text{const.}$ Defining the current density as $\mathbf{J} = \nabla \times \mathbf{B}$, it has the unit of inverse time. The electric field has then the unit of squared velocity. Furthermore, ν is the kinematic viscosity and η the magnetic diffusivity.

As will become clear, the major difficulty in defining a test-field method for MHD or purely magnetic background turbulence is caused by bilinear (or quadratic) terms like $\mathbf{J} \times \mathbf{B}$ and $\mathbf{U} \times \mathbf{B}$. Hence, taking the $\mathbf{U} \cdot \nabla \mathbf{U}$ nonlinearity into account would not offer any new aspect, but would blur the essence of the derivation and the clear analogy in the treatment of the former two nonlinearities. The treatment of the advective term follows the same pattern, as is demonstrated in Appendix A. Also, it should be pointed out that working with the simpler set of equations helps reducing the risk of errors in the numerical implementation.

In three dimensions and for $\mathbf{B}_{\text{imp}} = \mathbf{F}_M = \mathbf{0}$, but helical or non-helical kinetic forcing via \mathbf{F}_K , this system of

equations is capable of reproducing essential features of turbulent dynamos like initial exponential growth and subsequent saturation; see, e.g., Brandenburg (2001) or Haugen et al. (2004).

If $\mathbf{B}_{\text{imp}} \neq \mathbf{0}$ or $\mathbf{F}_M \neq \mathbf{0}$ we are no longer dealing with a dynamo problem in the strictest sense. A discussion of dynamo processes can still be meaningful if $\mathbf{B}_{\text{imp}} = \mathbf{0}$ and the magnetic forcing does not give rise to a mean electromotive force \mathcal{E}_0 . A possibility to accomplish this is $\mathbf{F}_K = \mathbf{0}$ together with a magnetic forcing resulting in a Beltrami field \mathbf{b}_0 , but any choice providing an isotropic background turbulence $\mathbf{b}_0, \mathbf{u}_0$ should be suited likewise.

Note that the mean-field induction equation is still autonomous allowing for the solution $\overline{\mathbf{B}} = \mathbf{0}$. It then depends on properties of the background turbulence like chirality whether, e.g., the α effect or other mean-field effects render this solution unstable by enabling growing solutions.

If we admit $\mathbf{B}_{\text{imp}} \neq \mathbf{0}$, the two forcing terms can in principle be adjusted such that the resulting background turbulence is again isotropic and $\overline{\mathcal{E}}_0 = \mathbf{0}$. Should a growing mean field then be observed, it can legitimately be attributed to an instability as $\overline{\mathbf{B}} = \mathbf{B}_{\text{imp}}$ is a solution of the mean field induction equation and the imposed field cannot grow. Thus both scenarios have the potential to exhibit *mean-field* dynamos although the original induction equation is inhomogeneous and the dynamo must not be considered as an instability of the completely non-magnetic state.

Models of the latter type may well have astrophysical relevance, because at high magnetic Reynolds numbers small-scale dynamo action is expected to be ubiquitous. Large-scale fields are still considered to be the consequence of an instability, at least if there is no $\overline{\mathcal{E}}_0$ or any other sort of “battery effect”. Magnetic forcing can be regarded as a modeling tool for providing a magnetic background turbulence when, e.g., in a DNS the conditions for small-scale dynamo action are not afforded.

More generally, magnetic forcing and an imposed field provide excellent means of studying the α effect, the inverse cascade of magnetic helicity, and flow properties in the magnetically dominated regime (see, e.g., Pouquet et al. 1976; Brandenburg et al. 2002; Brandenburg & Käpylä 2007).

3.2. Purely magnetic background turbulence

Before taking on the most general situation of both magnetic and velocity fluctuations in the background turbulence it seems instructive to look first at the case complementary to that discussed in Section 2. That is, we assume, perhaps somewhat artificially, that the background velocity fluctuations vanish, i.e. $\mathbf{u}_0 = \mathbf{0}$, so that $\mathbf{u} = \mathbf{u}_{\overline{\mathbf{B}}}$. According to (3) we now find

$$\overline{\mathcal{E}} = \overline{\mathcal{E}_{\overline{\mathbf{B}}}} = \overline{\mathbf{u}_{\overline{\mathbf{B}}} \times \mathbf{b}} = \overline{\mathbf{u} \times \mathbf{b}}. \quad (12)$$

The modified momentum equation for the velocity fluctuations in a homogeneous medium reads (cf. (10))

$$\frac{\partial \mathbf{u}}{\partial t} = \overline{\mathbf{J}} \times \mathbf{b} + \mathbf{j} \times \overline{\mathbf{B}} + \mathcal{F}' + \nu \nabla^2 \mathbf{u}, \quad (13)$$

with $\mathcal{F}' = \mathbf{j}_{\overline{\mathbf{B}}} \times \mathbf{b} + \mathbf{j}_0 \times \mathbf{b}_{\overline{\mathbf{B}}} - \overline{\mathbf{j}_{\overline{\mathbf{B}}} \times \mathbf{b}} + \overline{\mathbf{j}_0 \times \mathbf{b}_{\overline{\mathbf{B}}}}$. As $(\mathbf{j}_0 \times \mathbf{b}_0)'$ needs to vanish in order to guarantee $\mathbf{u}_0 = \mathbf{0}$, this could

also be written as $\mathcal{F}' = \mathbf{j} \times \mathbf{b} - \overline{\mathbf{j} \times \mathbf{b}}$. Unlike in the quasi-kinematic method there is now no longer any way to base a test-field method upon considering one of the fluctuating fields, here \mathbf{b} , to be given (e.g. taken from a main run) while interpreting the other, here \mathbf{u} , as a linear and homogeneous functional of the mean field. (This would work here, however, in the second order correlation approximation, where \mathcal{F}' is set to zero.)

3.3. General mean-field treatment

The mean-field equations for $\overline{\mathbf{U}}$ and $\overline{\mathbf{B}} = \text{curl} \overline{\mathbf{A}} + \mathbf{B}_{\text{imp}}$ obtained by averaging Eqs. (10) and (11) are

$$\frac{\partial \overline{\mathbf{U}}}{\partial t} = \nu \nabla^2 \overline{\mathbf{U}} + \overline{\mathbf{J}} \times \overline{\mathbf{B}} + \overline{\mathcal{F}}, \quad (14)$$

$$\frac{\partial \overline{\mathbf{A}}}{\partial t} = \eta \nabla^2 \overline{\mathbf{A}} + \overline{\mathbf{U}} \times \overline{\mathbf{B}} + \overline{\mathcal{E}}, \quad (15)$$

where we have assumed that the mean forcing terms vanish. From now on we extend our considerations also onto the relation between the mean force $\mathcal{F} = \mathbf{j} \times \mathbf{b}$ and the mean field. In full analogy to the mean electromotive force we find this relation, considered as a functional of $\mathbf{u}, \overline{\mathbf{U}}$ and $\overline{\mathbf{B}}$, again to be linear and homogeneous in the latter and write, to start with,

$$\overline{\mathcal{F}_{\overline{\mathbf{B}}}} = \phi \overline{\mathbf{B}} - \psi \nabla \overline{\mathbf{B}}. \quad (16)$$

Like α and η , the tensors ϕ and ψ may depend on $\overline{\mathbf{B}}$. In the kinematic limit ϕ and ψ are expected to be non-vanishing only if $\mathbf{b}_0 \neq \mathbf{0}$. An analysis in SOCA, however, would also require $\mathbf{u}_0 \neq \mathbf{0}$ to get a non-vanishing result; see Appendix B. Note that $\mathbf{b}_0 \neq \mathbf{0}$ allows $\overline{\mathcal{F}_{\overline{\mathbf{B}}}}$ to be linear in $\overline{\mathbf{B}}$, which would otherwise be quadratic to leading order. Consequently, the backreaction of the mean field onto the flow is no longer independent of its sign.

As $\overline{\mathcal{F}_{\overline{\mathbf{B}}}}$ is the divergence of the mean Maxwell tensor, it has to vanish in the homogeneous case, i.e. for homogeneous turbulence and a uniform field. Hence, for Equation (16) to be valid in physical space, ϕ has then to vanish. However, in Fourier space we may retain relation (16) with $\lim_{\mathbf{k} \rightarrow \mathbf{0}} \phi(\mathbf{k}) = \mathbf{0}$ (but not so for ψ). On the other hand, in the physical space a description of $\overline{\mathcal{F}_{\overline{\mathbf{B}}}}$ employing the second derivative of $\overline{\mathbf{B}}$ is likely to be more appropriate, i.e.

$$\overline{\mathcal{F}_{\overline{\mathbf{B}}}} = \phi^* \nabla^2 \overline{\mathbf{B}} - \psi \nabla \overline{\mathbf{B}}. \quad (17)$$

According to the expression for $\phi(\mathbf{k})$, which is derived in Appendix B for Roberts forcing, Equation (17) specified to

$$\overline{\mathcal{F}_{\overline{\mathbf{B}}}} = \phi^* \frac{\partial^2 \overline{\mathbf{B}}}{\partial z^2} - \psi \overline{\mathbf{J}}$$

would indeed be sufficient as long as there is sufficient scale separation between mean and fluctuating fields. In the following, we continue referring to ϕ as introduced by Equation (16).

The equations for the fluctuations are obtained by subtracting (14) from (10), and (15) from (11), what leads to

$$\frac{\partial \mathbf{u}}{\partial t} = \overline{\mathbf{J}} \times \mathbf{b} + \mathbf{j} \times \overline{\mathbf{B}} + \mathcal{F}' + \mathbf{f}_K + \nu \nabla^2 \mathbf{u}, \quad (18)$$

$$\frac{\partial \mathbf{a}}{\partial t} = \overline{\mathbf{U}} \times \mathbf{b} + \mathbf{u} \times \overline{\mathbf{B}} + \mathcal{E}' + \mathbf{f}_M + \eta \nabla^2 \mathbf{a}, \quad (19)$$

respectively, where $\mathcal{F}' = \mathbf{j} \times \mathbf{b} - \overline{\mathbf{j} \times \mathbf{b}}$ and $\mathcal{E}' = \mathbf{u} \times \mathbf{b} - \overline{\mathbf{u} \times \mathbf{b}}$ are terms that are quadratic in the correlations, while $\mathbf{f}_{K,M}$ are just the fluctuating parts of the forcing functions.

To arrive at a set of equations that are formally linear and allow for solutions as responses to a given mean field that are formally linear and homogeneous in the latter we make use of the split of all quantities into parts existing in the absence of $\overline{\mathbf{B}}$ and parts vanishing with $\overline{\mathbf{B}}$ introduced in Sect. 2. We write $\mathbf{u} = \mathbf{u}_0 + \mathbf{u}_{\overline{\mathbf{B}}}$, $\mathbf{a} = \mathbf{a}_0 + \mathbf{a}_{\overline{\mathbf{B}}}$ and $\mathbf{j} = \mathbf{j}_0 + \mathbf{j}_{\overline{\mathbf{B}}}$, further $\mathcal{F}' = \mathcal{F}'_0 + \mathcal{F}'_{\overline{\mathbf{B}}}$ and $\mathcal{E}' = \mathcal{E}'_0 + \mathcal{E}'_{\overline{\mathbf{B}}}$ and assume that the forcing is independent of $\overline{\mathbf{B}}$. Equation (18) and (19) split consequently as follows (see Appendix C for an illustration)

$$\frac{\partial \mathbf{u}_0}{\partial t} = \nu \nabla^2 \mathbf{u}_0 + \mathcal{F}'_0 + \mathbf{f}_K, \quad (20)$$

$$\frac{\partial \mathbf{a}_0}{\partial t} = \eta \nabla^2 \mathbf{a}_0 + \overline{\mathbf{U}} \times \mathbf{b}_0 + \mathcal{E}'_0 + \mathbf{f}_M, \quad (21)$$

$$\frac{\partial \mathbf{u}_{\overline{\mathbf{B}}}}{\partial t} = \nu \nabla^2 \mathbf{u}_{\overline{\mathbf{B}}} + \overline{\mathbf{J}} \times \mathbf{b} + \mathbf{j} \times \overline{\mathbf{B}} + \mathcal{F}'_{\overline{\mathbf{B}}}, \quad (22)$$

$$\frac{\partial \mathbf{a}_{\overline{\mathbf{B}}}}{\partial t} = \eta \nabla^2 \mathbf{a}_{\overline{\mathbf{B}}} + \overline{\mathbf{U}} \times \mathbf{b}_{\overline{\mathbf{B}}} + \mathbf{u} \times \overline{\mathbf{B}} + \mathcal{E}'_{\overline{\mathbf{B}}}. \quad (23)$$

Because of $\mathcal{F}'_0 = (\mathbf{j}_0 \times \mathbf{b}_0)'$ and $\mathcal{E}'_0 = (\mathbf{u}_0 \times \mathbf{b}_0)'$, Eqs. (20) and (21) are completely closed. Furthermore, we have

$$\mathcal{F}'_{\overline{\mathbf{B}}} = (\mathbf{j}_0 \times \mathbf{b}_{\overline{\mathbf{B}}} + \mathbf{j}_{\overline{\mathbf{B}}} \times \mathbf{b}_0 + \mathbf{j}_{\overline{\mathbf{B}}} \times \mathbf{b}_{\overline{\mathbf{B}}})', \quad (24)$$

$$\mathcal{E}'_{\overline{\mathbf{B}}} = (\mathbf{u}_0 \times \mathbf{b}_{\overline{\mathbf{B}}} + \mathbf{u}_{\overline{\mathbf{B}}} \times \mathbf{b}_0 + \mathbf{u}_{\overline{\mathbf{B}}} \times \mathbf{b}_{\overline{\mathbf{B}}})'. \quad (25)$$

We can rewrite these expressions such that they become formally linear in $\mathbf{u}_{\overline{\mathbf{B}}}$ and $\mathbf{b}_{\overline{\mathbf{B}}}$ each in two different flavors:

$$\mathcal{F}'_{\overline{\mathbf{B}}} = (\mathbf{j} \times \mathbf{b}_{\overline{\mathbf{B}}} + \mathbf{j}_{\overline{\mathbf{B}}} \times \mathbf{b}_0)' = (\mathbf{j}_0 \times \mathbf{b}_{\overline{\mathbf{B}}} + \mathbf{j}_{\overline{\mathbf{B}}} \times \mathbf{b})', \quad (26)$$

$$\mathcal{E}'_{\overline{\mathbf{B}}} = (\mathbf{u} \times \mathbf{b}_{\overline{\mathbf{B}}} + \mathbf{u}_{\overline{\mathbf{B}}} \times \mathbf{b}_0)' = (\mathbf{u}_0 \times \mathbf{b}_{\overline{\mathbf{B}}} + \mathbf{u}_{\overline{\mathbf{B}}} \times \mathbf{b})'. \quad (27)$$

Now we have achieved our goal of deriving a system of formally linear equations defining the part of the fluctuations that can be related to the mean field as response to the interaction with the given fluctuating fields \mathbf{u} , \mathbf{u}_0 , \mathbf{b} , and \mathbf{b}_0 .

Splitting mean force and electromotive force we find

$$\overline{\mathcal{F}}_0 = \overline{\mathbf{j}_0 \times \mathbf{b}_0} \quad \text{and} \quad \overline{\mathcal{E}}_0 = \overline{\mathbf{u}_0 \times \mathbf{b}_0} \quad (28)$$

for the parts existing already with $\overline{\mathbf{B}} = \mathbf{0}$, due to a small-scale dynamo or magnetic forcing. Although it is hard to imagine that isotropic forcing alone is capable of enabling a non-vanishing $\overline{\mathcal{E}}_0$, an additional vector influencing the otherwise isotropic turbulence may well act in this way. For example, using the second-order correlation approximation (SOCA) it was found that in the presence of a non-uniform mean flow $\overline{\mathbf{U}}$, with mean vorticity $\overline{\mathbf{W}} = \text{curl } \overline{\mathbf{U}}$, we have in ideal MHD ($\eta = \nu = 0$)

$$\overline{\mathcal{E}}_0 = -\frac{\tau_U}{3} \overline{\mathbf{u}_0 \cdot \mathbf{j}_0} \overline{\mathbf{U}} + \frac{\tau_W}{3} \overline{\mathbf{u}_0 \cdot \mathbf{b}_0} \overline{\mathbf{W}}. \quad (29)$$

Here the index "0" refers to the fluctuating background uninfluenced by both the magnetic field and the mean flow. Beyond this specific result, too, one may expect that some cross correlation of the primary turbulences is crucial. (Yoshizawa 1990; Rädler & Brandenburg 2010).

For the parts vanishing with $\overline{\mathbf{B}}$ we have

$$\overline{\mathcal{F}}_{\overline{\mathbf{B}}} = \overline{\mathbf{j} \times \mathbf{b}_{\overline{\mathbf{B}}} + \mathbf{j}_{\overline{\mathbf{B}}} \times \mathbf{b}_0} = \overline{\mathbf{j}_0 \times \mathbf{b}_{\overline{\mathbf{B}}} + \mathbf{j}_{\overline{\mathbf{B}}} \times \mathbf{b}}, \quad (30)$$

$$\overline{\mathcal{E}}_{\overline{\mathbf{B}}} = \overline{\mathbf{u} \times \mathbf{b}_{\overline{\mathbf{B}}} + \mathbf{u}_{\overline{\mathbf{B}}} \times \mathbf{b}_0} = \overline{\mathbf{u}_0 \times \mathbf{b}_{\overline{\mathbf{B}}} + \mathbf{u}_{\overline{\mathbf{B}}} \times \mathbf{b}}. \quad (31)$$

We recall that for $\mathbf{b}_0 = \mathbf{0}$ (see Section 2), only the term $\overline{\mathbf{u} \times \mathbf{b}_{\overline{\mathbf{B}}}} \equiv \overline{\mathcal{E}}_{\overline{\mathbf{B}}}^K$ occurs in the mean electromotive force and for $\mathbf{u}_0 = \mathbf{0}$ (see Equation (12)) only $\overline{\mathbf{u}_{\overline{\mathbf{B}}} \times \mathbf{b}} \equiv \overline{\mathcal{E}}_{\overline{\mathbf{B}}}^M$. For interpretation purposes, it is therefore convenient to define a correspondingly symmetrized version,

$$\overline{\mathcal{F}}_{\overline{\mathbf{B}}} = \overline{\mathbf{j} \times \mathbf{b}_{\overline{\mathbf{B}}} + \mathbf{j}_{\overline{\mathbf{B}}} \times \mathbf{b} - \mathbf{j}_{\overline{\mathbf{B}}} \times \mathbf{b}_{\overline{\mathbf{B}}}} = \overline{\mathcal{F}}_{\overline{\mathbf{B}}}^K + \overline{\mathcal{F}}_{\overline{\mathbf{B}}}^M + \overline{\mathcal{F}}_{\overline{\mathbf{B}}}^R$$

$$\overline{\mathcal{E}}_{\overline{\mathbf{B}}} = \overline{\mathbf{u} \times \mathbf{b}_{\overline{\mathbf{B}}} + \mathbf{u}_{\overline{\mathbf{B}}} \times \mathbf{b} - \mathbf{u}_{\overline{\mathbf{B}}} \times \mathbf{b}_{\overline{\mathbf{B}}}} = \overline{\mathcal{E}}_{\overline{\mathbf{B}}}^K + \overline{\mathcal{E}}_{\overline{\mathbf{B}}}^M + \overline{\mathcal{E}}_{\overline{\mathbf{B}}}^R,$$

with $\overline{\mathcal{F}}_{\overline{\mathbf{B}}}^R = -\overline{\mathbf{j}_{\overline{\mathbf{B}}} \times \mathbf{b}_{\overline{\mathbf{B}}}}$ and $\overline{\mathcal{E}}_{\overline{\mathbf{B}}}^R = -\overline{\mathbf{u}_{\overline{\mathbf{B}}} \times \mathbf{b}_{\overline{\mathbf{B}}}}$ being residual terms. Of course this split is only meaningful with a non-vanishing mean field in the main run. The corresponding transport coefficients might be split analogously. Note, however, that for an imposed field in, say, the x direction this is restricted to the $(1j)$ components of the tensors.

3.4. Test-field method

In a next step we define the actual test equations starting from Eqs. (22), (23), (26) and (27). As they are already arranged to be formally linear when deliberately ignoring the relations between $\mathbf{u}_{\overline{\mathbf{B}}}$ and \mathbf{u} as well as between $\mathbf{b}_{\overline{\mathbf{B}}}$ and \mathbf{b} , respectively, we have nothing more to do than to identify $\overline{\mathbf{B}}$ with a test field $\overline{\mathbf{B}}^T$ and $\mathbf{b}_{\overline{\mathbf{B}}}, \mathbf{u}_{\overline{\mathbf{B}}}$ with the corresponding test solutions $\mathbf{b}^T, \mathbf{u}^T$. Due to the ambiguity in (26) and (27) four different versions are obtained reading

$$\frac{\partial \mathbf{u}^T}{\partial t} = \overline{\mathcal{F}}^T \times \mathbf{b} + \mathbf{j} \times \overline{\mathbf{B}}^T + \mathcal{F}'_T + \nu \nabla^2 \mathbf{u}^T, \quad (32)$$

$$\frac{\partial \mathbf{a}^T}{\partial t} = \overline{\mathcal{E}}^T \times \mathbf{b} + \mathbf{u} \times \overline{\mathbf{B}}^T + \mathcal{E}'_T + \eta \nabla^2 \mathbf{a}^T, \quad (33)$$

with

$$\overline{\mathcal{F}}^T = \begin{cases} (\mathbf{j} \times \mathbf{b}^T + \mathbf{j}^T \times \mathbf{b}_0)' \\ \text{or} \\ (\mathbf{j}_0 \times \mathbf{b}^T + \mathbf{j}^T \times \mathbf{b})', \end{cases} \quad (34)$$

$$\overline{\mathcal{E}}^T = \begin{cases} (\mathbf{u} \times \mathbf{b}^T + \mathbf{u}^T \times \mathbf{b}_0)' \\ \text{or} \\ (\mathbf{u}_0 \times \mathbf{b}^T + \mathbf{u}^T \times \mathbf{b})'. \end{cases} \quad (35)$$

For mean force and electromotive force expressed by the test solutions we write correspondingly

$$\overline{\mathcal{F}}^T = \begin{cases} \overline{\mathbf{j} \times \mathbf{b}^T + \mathbf{j}^T \times \mathbf{b}_0} \\ \text{or} \\ \overline{\mathbf{j}_0 \times \mathbf{b}^T + \mathbf{j}^T \times \mathbf{b}}, \end{cases} \quad (36)$$

$$\overline{\mathcal{E}}^T = \begin{cases} \overline{\mathbf{u} \times \mathbf{b}^T + \mathbf{u}^T \times \mathbf{b}_0} \\ \text{or} \\ \overline{\mathbf{u}_0 \times \mathbf{b}^T + \mathbf{u}^T \times \mathbf{b}}, \end{cases} \quad (37)$$

and stipulate that the choice within Eqs. (36) and (37) is always to correspond to the choice in Eqs. (34) and (35).

Table 1. Illustration of generating the four versions of the generalized test-field method by combining the different ways of representing \mathcal{F}'_T and \mathcal{E}'_T in Eqs. (34) and (35)

	$\mathbf{j} \times \mathbf{b}^T + \mathbf{j}^T \times \mathbf{b}_0$	$\mathbf{j}_0 \times \mathbf{b}^T + \mathbf{j}^T \times \mathbf{b}$
$\mathbf{u} \times \mathbf{b}^T + \mathbf{u}^T \times \mathbf{b}_0$	ju	bu
$\mathbf{u}_0 \times \mathbf{b}^T + \mathbf{u}^T \times \mathbf{b}$	jb	bb

As we will make use of all four possible versions we label them in a unique way by the names of the fluctuating fields of the main run that enter the expressions for \mathcal{F}'_T and \mathcal{E}'_T . Accordingly, we find by inspection of Eqs. (34) and (35) for the labels the combinations ju, jb, bu and bb; see Table 1.

Now we conclude that for given \mathbf{u} , \mathbf{b} , \mathbf{u}_0 , \mathbf{b}_0 and $\bar{\mathbf{U}}$ the test solutions \mathbf{u}^T , \mathbf{b}^T are linear and homogeneous in the test fields $\bar{\mathbf{B}}^T$ and that the same holds for $\bar{\mathcal{F}}^T$ and $\bar{\mathcal{E}}^T$. Hence, the tensors α , η , ϕ and ψ derived from these quantities will not depend on the test fields, but exclusively reflect properties of the given fluctuating fields and the mean velocity. If these are affected by a mean field in the main run the tensor components will show a dependence on $\bar{\mathbf{B}}$. Thus, like in the quasi-kinematic method, quenching behavior can be identified. We observe further that when using the mean field from the main run as one of the test fields, the corresponding test solutions \mathbf{b}^T and \mathbf{u}^T will coincide with $\mathbf{b} - \mathbf{b}_0$ and $\mathbf{u} - \mathbf{u}_0$, respectively.

Summing up, we may claim that the presented generalized test-field method in either shape satisfies certain necessary conditions for the correctness of its results. But can we be confident, that these are sufficient, too? An obvious complication lies in the fact, that in contrast to the quasi-kinematic method yielding the transport coefficients uniquely, we have now to deal with four different versions which need not be completely equivalent. Indeed we will demonstrate that the reformulation of the original problem into Eqs. (32) and (33) with Eqs. (34) and (35) introduces occasional spurious instabilities. As we presently see no strict mathematical argument for the identity of the outcomes of all four versions, we resort to an empirical justification of our approach. This is what the rest of this paper is devoted to.

Remarks: (i) Applying the second order correlation approximation (SOCA) to the system (32), (33), that is, neglecting \mathcal{F}'_T and \mathcal{E}'_T , melts the four versions down to one and thus removes all complications.

(ii) In the limit $\bar{\mathbf{B}} \rightarrow \mathbf{0}$ we have simultaneously $\mathbf{u} \rightarrow \mathbf{u}_0$ and $\mathbf{b} \rightarrow \mathbf{b}_0$, so again only one version remains. The method has then of course no longer any value for quenching considerations, but it still might be useful to overcome the limitations of SOCA.

(iii) For $\mathbf{b}_0 = \mathbf{0}$ the \mathbf{a}^T equation (33) with the first version of (35), i.e.

$$\mathcal{E}'_T = (\mathbf{u} \times \mathbf{b}_T)'$$
(38)

and correspondingly $\bar{\mathcal{E}}_T = \overline{\mathbf{u} \times \mathbf{b}_T}$, but (32) ignored, reverts to the quasi-kinematic method. For comparison we will occasionally apply this method even when $\mathbf{b}_0 \neq \mathbf{0}$ and label the quantities calculated in this way with an upper index “QK”.

From now on we define mean fields by averaging over two directions, here over the x and y directions, that is, all mean quantities depend merely on z (if at all) and we get a 1D mean-field dynamo problem. As a consequence, \bar{B}_z is constant and there are only two non-vanishing components of $\nabla \bar{\mathbf{B}}$, namely \bar{J}_x and \bar{J}_y so only the evolution of \bar{B}_x and \bar{B}_y has to be considered. Moreover, $\bar{\mathcal{E}}_z$ is without influence on the evolution of $\bar{\mathbf{B}}$. Hence, instead of Eqs. (16) and (8) we can write

$$\bar{\mathcal{F}}_i = \phi_{ij} \bar{B}_j - \psi_{ij} \bar{J}_j, \quad \bar{\mathcal{E}}_i = \alpha_{ij} \bar{B}_j - \eta_{ij} \bar{J}_j, \quad (39)$$

where the original rank-three tensors ψ and η are degenerated to rank-two ones.

Only the four components of either tensor with $i, j = 1, 2$ are of interest, thus altogether 16 components need to be determined. As one test field $\bar{\mathbf{B}}^T$ comprises two relevant components and yields an $\bar{\mathcal{F}}^T$ and an $\bar{\mathcal{E}}^T$, each again with two relevant components, we need to consider solutions of Eqs. (22) and (23) with Eqs. (34) and (35) for a set of four different test fields.

Selection of test fields: The simplest choice are homogeneous fields in the x and y directions, but they are only suited to determine the α tensor.

All four tensors can be extracted by use of test fields with either the x or the y component proportional to either $\cos kz$ or to $\sin kz$ and the other vanishing (see, e.g., Brandenburg 2005b; Brandenburg et al. 2008a, 2008b; Sur et al. 2008). That is, $\bar{\mathbf{B}}^T$ is either $B_i^{pc} = \delta_{ip} \cos kz$ or $B_i^{ps} = \delta_{ip} \sin kz$, $p = 1, 2$, where the superscript pq , $q = c, s$ labels the test field and the subscript i refers to its components. By varying the wavenumber k , the wanted tensor components can in principle be determined as functions of k , but are then no longer allowed to be interpreted in the usual way (cf. Brandenburg et al. 2008a). Here we refrain from doing so and fix k to the smallest possible value $k = 2\pi/L_z$ where L_z is the extent of the computational domain in z direction. But even then we introduce some errors because the harmonic test fields do not belong to the class of mean fields for which the ansatzes Eqs. (16) and (8) are exhaustive (see Sect. 2). We must be aware that the tensors calculated in this way are “polluted” by some contributions from terms with higher derivatives of $\bar{\mathbf{B}}$ in $\bar{\mathcal{E}}$ and $\bar{\mathcal{F}}$. To monitor these departures we compare the α and ϕ tensors found with harmonic test fields with those obtained with uniform ones.

For each pair of test fields (B^{pc} , B^{ps}) we determine 2×4 unknowns by solving the linear systems

$$\bar{\mathcal{F}}_i^{pq} = \phi_{ij} \bar{B}_j^{pq} - \psi_{ij} \bar{J}_j^{pq}, \quad \bar{\mathcal{E}}_i^{pq} = \alpha_{ij} \bar{B}_j^{pq} - \eta_{ij} \bar{J}_j^{pq}. \quad (40)$$

$q = c, s$. Note that there is no coupling between the systems for $p = 1$ and $p = 2$. Inversion of the rotation matrix

$$\mathbf{R} = \begin{pmatrix} \cos kz & -\sin kz \\ \sin kz & \cos kz \end{pmatrix} \quad (41)$$

(with the angle kz) provides the solutions explicitly, hence we have

$$\begin{pmatrix} \phi_{ij} \\ \psi_{ij} k \end{pmatrix} = \mathbf{R}^t \begin{pmatrix} \bar{\mathcal{F}}_i^{jc} \\ \bar{\mathcal{F}}_i^{js} \end{pmatrix}, \quad \begin{pmatrix} \alpha_{ij} \\ \eta_{ij} k \end{pmatrix} = \mathbf{R}^t \begin{pmatrix} \bar{\mathcal{E}}_i^{jc} \\ \bar{\mathcal{E}}_i^{js} \end{pmatrix}. \quad (42)$$

Here the superscript “t” indicates transposition.

3.5. Forcing functions, computational domains and boundary conditions

For testing purposes, a common and convenient choice is the Roberts flow forcing function,

$$\mathbf{f} = \sigma k_f \Psi \hat{\mathbf{z}} + \nabla \times (\Psi \hat{\mathbf{z}}) \quad \text{with} \quad \Psi = \cos k_x x \cos k_y y, \quad (43)$$

and the effective forcing wavenumber $k_f = (k_x^2 + k_y^2)^{1/2}$. With the chosen averaging the Roberts forcing is isotropic in the xy plane. Furthermore, σ is a parameter controlling the helicity of the flow: with $\sigma = 0$ it is non-helical while for $\sigma = 1$ it reaches maximum helicity. If not declared otherwise, we will employ just maximally helical Roberts forcing.

The Roberts forcing function can be employed for kinetic as well as magnetic forcing, so we write $\mathbf{f}_{K,M} = N_{K,M} \mathbf{f}$, where the $N_{K,M}$ are amplitudes having the units of acceleration and velocity squared, respectively. Note that for $\sigma = 1$ Eq. (43) yields a Beltrami field, i.e., it has the property $\text{curl} \mathbf{f} = k_f \mathbf{f}$. Therefore, provided $\mathbf{B}_{\text{imp}} = \mathbf{0}$, kinetic and magnetic forcing act completely uninfluenced from each other and create just a flow and a magnetic field having exactly the Roberts geometry. This is not the case for $\sigma \neq 1$.

The computational domain is a cuboid with quadratic base $L_x = L_y = 2\pi$ while its z extent remains adjustable and depends on the smallest wavenumber in the z direction, k_{1z} , to be considered. However, as the Roberts forcing function is not z dependent, the runs from which only α and ϕ are extracted were carried out in 2D with $k_{1z} = 0$.

We choose here $k_x = k_y = k_1$ where $k_1 = 1$ is the smallest wavenumber that fits into x and y extent of the computational domain. For random forcing the domain is always cubic, i.e. $L_x = L_y = L_z = 2\pi$. In all cases we assume periodic boundary conditions in all directions. The results presented below are based on revision **r13439** of the PENCIL CODE¹, which is a modular high-order code (sixth order in space and third-order in time) for solving a large range of different partial differential equations.

3.6. Control parameters and non-dimensionalization

In cases with an imposed magnetic field, we set $\mathbf{B}_{\text{imp}} = (B_0, 0, 0)$. Along with it the forcing amplitudes $N_{K,M}$ are the most relevant control parameters. The only remaining one is the magnetic Prandtl number, $\text{Pr}_M = \nu/\eta$.

It is convenient to measure length in units of the inverse minimal wavenumber k_1 , time in units of $1/\eta k_1^2$, velocity in units of ηk_1 , and the magnetic field also in units of ηk_1 . The forcing amplitudes $N_{K,M}$ are given in units of $\eta^2 k_1^3$ and $\eta^2 k_1^2$, respectively. Results will also be presented in dimensionless form: α_{ij} and ψ_{ij} in units of ηk_1 , η_{ij} in units of η , ϕ_{ij} in units of ηk_1^2 if not declared otherwise. Dimensionless quantities are denoted by a tilde throughout.

The intensities of the physically relevant actual and primary turbulences are readily measured by the magnetic Reynolds number and the Lundquist number,

$$\text{Re}_M = u_{\text{rms}}/\eta k_f, \quad \text{Lu} = b_{\text{rms}}/\eta k_f, \quad (44)$$

where u_{rms} and b_{rms} are the rms values of fluctuating velocity and magnetic field, respectively, and k_f is the effective forcing wavenumber.

4. Results

Throughout this section we set the mean flow $\bar{\mathbf{U}}$ to zero. An important criterion for the correctness of the generalized test-field methods is the agreement of their results with those of the imposed-field method. In most cases we checked for this criterion. Of course, the imposed-field method is only applicable if the actual mean field in the main run is uniform. If this is not the case, we are in some instances still able to perform validation by comparing with analytical results.

4.1. Zero mean magnetic field

In this section we assume that the mean field is absent or weak enough as not to affect the fluctuating fields markedly, that is, $\mathbf{u} \approx \mathbf{u}_0$, $\mathbf{b} \approx \mathbf{b}_0$. In particular it can then not render the transport coefficients anisotropic. Therefore, we denote by α and η_t simply the average of the first two diagonal components of α and η , i.e. $\alpha = (\alpha_{11} + \alpha_{22})/2$ and $\eta_t = (\eta_{11} + \eta_{22})/2$, respectively. If not specified otherwise we set $\tilde{B}_{\text{imp}} = 10^{-3}$ or zero. Furthermore, we take $\text{Pr}_M = 1$, i.e. $\nu = \eta$.

4.1.1. Purely hydrodynamic forcing

In order to make contact with known results, we consider first the case of the hydrodynamically driven Roberts flow. In two dimensions, no small-scale dynamo is possible, hence $\mathbf{b}_0 = \mathbf{0}$ and $u_{0\text{rms}} = N_K/\nu k_f^2$. In three dimensions, however, this solution could be unstable, but we have not yet employed sufficiently large Re_M allowing for that. For $\text{Re}_M \ll 1$, α is given by (Brandenburg et al. 2008a)

$$\alpha/\alpha_0K = \text{Re}_M/[1 + (k_z/k_f)^2], \quad \alpha_0K = -u_{\text{rms}}/2, \quad (45)$$

where k_z is the wavenumber of the harmonic test fields. The minus sign in α_0 accounts for the fact that the Roberts flow has positive helicity, which results in a negative α .

Making use of the quasi-kinematic method, as well as of all four versions of the generalized method, we calculated α for $N_M = 0$, $k_z = 0$ (2D case) and values of \tilde{N}_K ranging from 0.01 to 100 with a ratio of 10; \tilde{u}_{rms} grows then from 0.005 to 50. Figure 1 shows α/α_0 versus Re_M (solid line). Here the data points for all methods are indistinguishable. All results also agree with those of the imposed-field method.

Agreement with the SOCA result (45) (dotted line) exists for $\text{Re}_M \ll 1$. For $\text{Re}_M > 1$, this is not applicable, because dropping the \mathcal{E}'_T term is then no longer justified. The SOCA values are nevertheless numerically reproducible by the test-field methods when ignoring the \mathcal{F}'_T and \mathcal{E}'_T terms in Eqs. (32) and (33); see the diamond-shaped data points in Figure 1.

Corrections to the result (45) with the \mathcal{E}'_T term retained were computed analytically by Rädler et al. (2002a,b). The corresponding values are again well reproduced by all flavors of the generalized test-field method as well as by the imposed-field method.

In the first line of Table 2, we repeat the result for $\tilde{N}_K = 1$ and added that for test fields with the wavenumber $k_z = 1$, from where we also come to know the turbulent diffusivity η_t . Note the difference between the α values for $k_z = 1$ and $k_z = 0$ roughly given by the factor $\sqrt{2}$ from

¹ <http://pencil-code.googlecode.com>

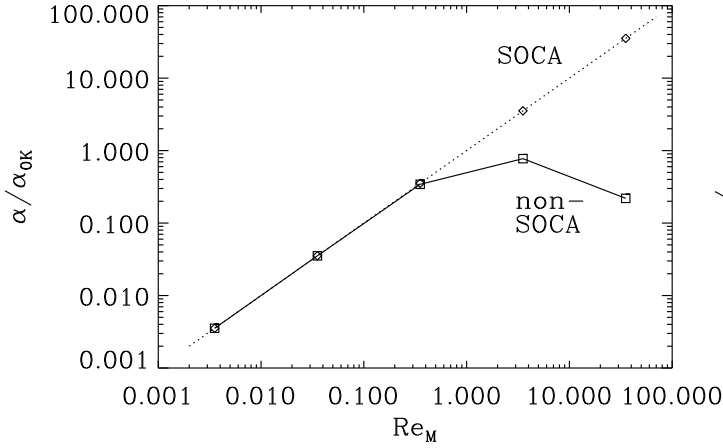


Fig. 1. α/α_{0K} vs. Re_M for purely kinetic Roberts forcing with $\text{Pr}_M = 1$ and $k_z = 0$ (2D case) from the quasi-kinematic and all versions of the generalized method (solid line with squares). Note the full agreement with Eq. (45) (dotted line) for $\text{Re}_M \ll 1$. Diamonds indicate the results of the test-field methods with the \mathcal{F}'_T and \mathcal{E}'_T terms in Eqs. (32) and (33) neglected, again coinciding with (45).

(45) for $k_z = k_f = 1$. Additionally, the results of the quasi-kinematic method for $k_z = 1$, α^{QK} and η_t^{QK} , are shown. As expected, they coincide completely with α and η_t .

4.1.2. Purely magnetic forcing

Next we consider the case of purely magnetic Roberts forcing i.e. $N_K = 0$. Due to its Beltrami property, $\mathbf{b}_0 \propto \mathbf{f}$, $\mathbf{u}_0 = \mathbf{0}$ is a solution of Eqs. (20) and (21). A bifurcation leading to solutions with $\mathbf{u}_0 \neq \mathbf{0}$ cannot be ruled out generally, but was never observed. Thus we have for the rms value of the magnetic vector potential $a_{0\text{rms}} = N_M/\eta k_f^2$, hence $b_{0\text{rms}} = N_M/\eta k_f$. The appropriate parameter for expressing the strength of the fluctuating field(s) is now the Lundquist number and the corresponding analytic result for $\text{Lu} \ll 1$ reads

$$\alpha/\alpha_{0M} = (\text{Lu}/\text{Pr}_M)/[1 + (k_z/k_f)^2], \quad \alpha_{0M} = 3b_{\text{rms}}/4 \quad (46)$$

(for the derivation see Appendix D). It turns out that the sign of α coincides now with that of the helicity of the forcing function. Again, we consider first the two-dimensional case with $k_z = 0$; see Figure 2. In analogy to purely hydrodynamic forcing we find for $\text{Lu} \ll 1$ agreement between all versions of the generalized test-field method (solid line with squares) with Equation (46) (dotted line). For higher values the SOCA versions (see Sect. 4.1.1) accomplish the same; see diamond data points. Note, that for the last data point with $\text{Lu} = 7$ it was necessary to lower the strength of the imposed field to $B_{\text{imp}}/\eta k_1 = 10^{-4}$, because otherwise the solution of the main run becomes unstable and changes to a new pattern.

The second line of Table 2 repeats the result for $\tilde{N}_M = 1$, again amended by those for $k_z = 1$ and the results of the quasi-kinematic method which is obviously unable to produce correct answers. This is because the mean electromotive force is now given by $\mathbf{u}_{\bar{B}} \times \mathbf{b}_0$, which is only taken into account in the generalized method. Note further that η_t is positive both for hydrodynamic and magnetic forcings.

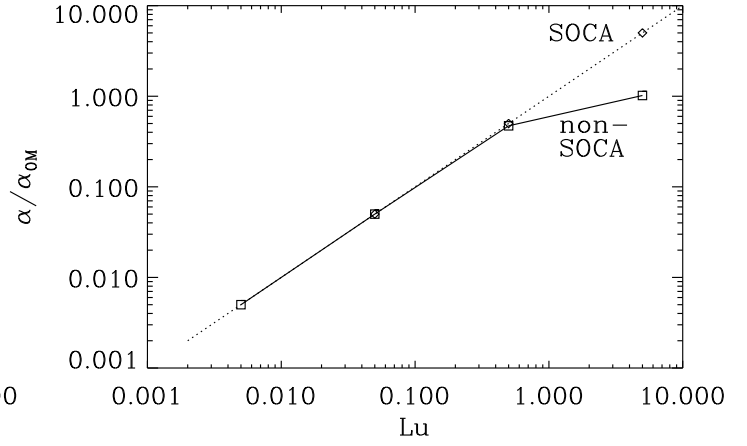


Fig. 2. α/α_{0M} versus Lu for purely magnetic Roberts forcing with $\text{Pr}_M = 1$ and $k_z = 0$ (2D case) from all versions of the generalized method (solid line with squares). Note the full agreement with Equation (46) (dotted line) for $\text{Lu} \ll 1$. Diamonds give the results of the test-field methods with the \mathcal{E}'_T and \mathcal{F}'_T terms in (38) neglected, again coinciding with (46).

Table 2. Kinematic results for $\tilde{\alpha}$ and $\tilde{\eta}_t$ for purely hydrodynamic ($\tilde{N}_M = 0$) purely magnetic ($\tilde{N}_K = 0$), and hydromagnetic Roberts forcing, $\text{Pr}_M = 1$. The wavenumber of the test field is $k_z = 1$, except in the third column where $k_z = 0$. Its results agree with those of the imposed-field method. $\tilde{\alpha}^{\text{QK}}$ and $\tilde{\eta}_t^{\text{QK}}$ refer to the quasi-kinematic method.

\tilde{N}_K	\tilde{N}_M	$\tilde{\alpha}(k_z = 0)$	$\tilde{\alpha}$	$\tilde{\alpha}^{\text{QK}}$	$\tilde{\eta}_t$	$\tilde{\eta}_t^{\text{QK}}$
1	0	-0.0857	-0.0569	-0.0569	0.0399	0.0399
0	1	0.2499	0.1684	0.0000	0.1188	0.0000
3.364	0	-0.7330	-0.4734	-0.4734	0.3087	0.3087
0	1.942	0.8219	0.5664	0.0000	0.3983	0.0000
3.364	1.942	-0.0081	0.0664	-0.4734	0.6604	0.3086
3.364	0	-1.0002	-0.6668	-0.6666	0.4715	0.4714 ¹
0	1.942	1.0000	0.6666	0.0000	0.4714	0.0000 ¹
3.364	1.942	$-4 \cdot 10^{-6}$	$2 \cdot 10^{-5}$	-0.6666	0.9428	0.4714 ¹

¹ with SOCA

4.1.3. Hydromagnetic forcing

As already pointed out in Sect. 3.5, in the absence of a mean field, for simultaneous kinetic and magnetic Roberts forcing there is a solution of Eqs. (20) and (21) consisting just of the solutions \mathbf{u}_0 and \mathbf{b}_0 of the system forced purely hydrodynamically and magnetically, respectively. Again, a bifurcation leading to another type of solution cannot be ruled out, but was not observed. Only within SOCA, however, the decoupling of \mathbf{u}_0 and \mathbf{b}_0 lets the value of α for hydromagnetic forcing be purely additive in the values for purely hydrodynamic and purely magnetic forcings. We denote the two latter by $\alpha_k = \alpha(\mathbf{b}_0 = \mathbf{0})$ and $\alpha_m = \alpha(\mathbf{u}_0 = \mathbf{0})$, respectively. When abandoning SOCA, the terms $(\mathbf{u}_{\bar{B}} \times \mathbf{b}_0)'$ and $(\mathbf{j}_0 \times \mathbf{b}_{\bar{B}} + \mathbf{j}_{\bar{B}} \times \mathbf{b}_0)'$ in Equations (22) and (23) provide couplings between $\mathbf{u}_{\bar{B}}$ and $\mathbf{b}_{\bar{B}}$ and give rise to an additional “magnetokinetic” part, of α defined as $\alpha_{\text{mk}} = \alpha - \alpha_k - \alpha_m$.

Note that we use here lower case subscripts k , m , and mk to distinguish from the split introduced at the end of Section 3.3, which applies to the nonlinear case. In contrast, the occurrence of α_{mk} is a purely kinematic effect. While α_k and α_m are, to leading order (and hence in SOCA), quadratic in the respective background fluctuations the magnetokinetic term is of leading fourth order and is representable in schematic form as $\alpha_{mk} \propto \langle \mathbf{u}_0 \psi_0 \mathbf{b}_0 \alpha_0 \rangle$.

Lines 5 and 8 of Table 2 show cases with hydromagnetic forcing and amplitudes adjusted such that we would have $\tilde{\alpha}_k = \tilde{\alpha}_m = 1$ if SOCA were valid. In either case the preceding two lines present the corresponding purely forced cases. Lines 6 to 8 refer to the SOCA version of the test-field methods. It can be clearly seen that the results are additive only in the latter case. The value of α_{mk} as inferred from lines 3 to 5 is -0.1 resulting in a considerable reduction of α in comparison with the purely additive value. This is owed to the strong forcing amplitudes leaving the applicability ranges of SOCA far behind.

Figure 3 shows α_{mk} for equally strong velocity and magnetic fluctuations as a function of $\text{Re}_M = \text{Lu}$ together with α_k , α_m , $\alpha_k + \alpha_m$ and the resulting total value α . Note the significant difference between the naive extrapolation of SOCA, $\alpha_m + \alpha_k$, and the true α . In its inset the figure shows the numerical values of α_{mk} in comparison to the result of a fourth order calculation $\alpha_{mk} = -\sqrt{2}/64 u_{\text{rms}}^2 b_{\text{rms}}^2$ (for the derivation see Appendix E). Clearly, the validity range of this expression extends beyond $\text{Re}_M = \text{Lu} = 1$ and hence further than the one of SOCA. It remains to be studied whether the magnetokinetic contribution has a significant effect also in the more general case when $\mathbf{u}_0 \nparallel \mathbf{b}_0$. If so, considering α to be the sum of a kinetic and a magnetic part, as often done in quenching considerations, may turn out to be too simplistic. Likewise one may wonder whether

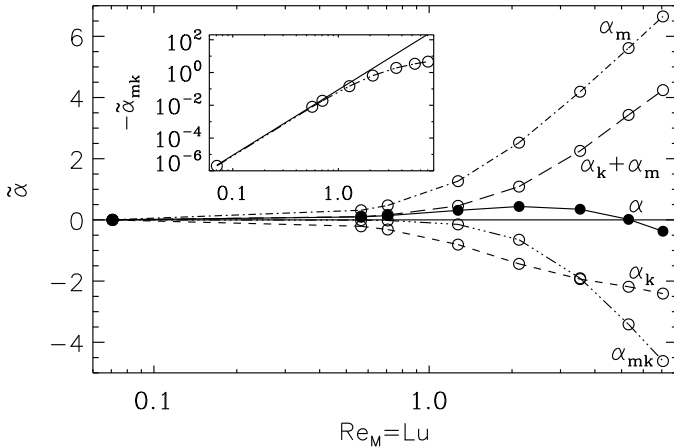


Fig. 3. α versus $\text{Re}_M = \text{Lu}$ for hydromagnetic Roberts forcing with $\text{Pr}_M = 1$ and $k_z = 0$ (2D case). Along with the total value the constituents α_k , α_m and α_{mk} as well as $\alpha_k + \alpha_m$ are shown. Note the sign change in α at $\text{Re}_M \approx 0.54$. The inset shows α_{mk} in comparison to the result of a fourth order analytical calculation (solid line).

closure approaches to the determination of transport coefficients supposed to be superior to SOCA can be successful at all as long as they do not take fourth order correlations into account properly.

For the tensors ϕ and ψ , which turn out to show up with simultaneous hydromagnetic and magnetic forcing only (in addition, ϕ requires z -dependent mean fields) we have of course again isotropy, $\phi_{11} = \phi_{22} \equiv \phi$, $\psi_{11} = \psi_{22} \equiv \psi$.

As a peculiarity of the Roberts flow, ψ vanishes in the range of validity of SOCA if the helicity is maximum ($\sigma = 1$ in (43)). For this case the first three panels of Figure 4 show the dependences $\alpha(k_z)$, $\eta(k_z)$ and $\phi(k_z)$ with different values of $u_{\text{rms}} = b_{\text{rms}}$ (data points, dotted lines). The last panel shows $\psi(k_z)$ for $\sigma = 0.5$ and the same forcing amplitudes as before. As explained above, \mathbf{u}_0 and \mathbf{b}_0 can now no longer be forced independently from each other. Hence both fields can not show exactly the geometry defined by (43) and u_{rms} and b_{rms} diverge increasingly with increasing forcing.

As demonstrated in Appendix B, $\phi(k_z) \propto k_z^2/(k_z^2 + k_f^2)$, $\alpha(k_z), \eta(k_z), \psi(k_z) \propto 1/(k_z^2 + k_f^2)$ in the SOCA limit. For comparison these functions are depicted by solid lines. Note the clear deviations from SOCA for $\text{Re}_M = \text{Lu} = 5$, particularly in α . Note also that the expression for ψ was derived under the assumption that the background has the geometry (43). It is therefore not applicable in a strict sense. The clear disagreement with the values of ψ from the test-field method for the high values of Re_M and Lu are hence not only due to violating the validity constraint $\text{Re}_M \ll 1$.

4.2. Dependence on the mean field

We now admit dynamically effective mean fields and hence have to deal with anisotropic fluctuating fields \mathbf{u} and \mathbf{b} which result in anisotropic tensors α , η , ϕ and ψ . For the chosen forcing, $\overline{\mathbf{B}}$ is the only source of anisotropy in the xy plane, so α has to have the form

$$\alpha_{ij} = \alpha_1 \delta_{ij} + \alpha_2 \hat{B}_i \hat{B}_j, \quad i, j = 1, 2,$$

with $\hat{\mathbf{B}}$ the unit vector in the direction of $\overline{\mathbf{B}}$ (here the x direction). We obtain then $\alpha_{11} = \alpha_1 + \alpha_2$ and $\alpha_{22} = \alpha_1$. Of course, the tensors η , ϕ and ψ are built analogously. Clearly, irrespective whether the forcing is pure or mixed the effects of B_{imp} prevent the fluctuating \mathbf{u} and \mathbf{b} from having Roberts geometry.

For vanishing magnetic background, $\mathbf{b}_0 = \mathbf{0}$, the generalized methods are still expected to give results coinciding with those of the quasi-kinematic one, but with $\mathbf{b}_0 \neq \mathbf{0}$ we will leave safe mathematical grounds and enter empirical work.

4.2.1. Purely hydrodynamic forcing

In this case we have $\overline{\mathcal{E}}_{\overline{\mathbf{B}}} = \overline{\mathbf{u} \times \mathbf{b}_{\overline{\mathbf{B}}}} = \overline{\mathcal{E}}_{\overline{\mathbf{B}}}^K$ and all flavors of the generalized method have to yield results which coincide with those of the quasi-kinematic method. This is valid to very high accuracy for the ju and bu versions and somewhat less perfectly so for the bb and jb versions. We emphasize that the presence of B_{imp} , although being solely responsible for the occurrence of magnetic fluctuations, does not result in a failure of the quasi-kinematic method as one might conclude from the model used by Courvoisier et al. (2010).

Figure 5 presents the constituents of α as functions of the imposed field in the 2D case with $\text{Pr}_M = 1$. We may conclude from the data that α_2 is negative and approximately equal to α_{11}^M . For values of $B_{\text{imp}}/\eta k_1 > 5$ its modulus approaches $\alpha_{22} = \alpha_1$ and thus gives rise to the strong

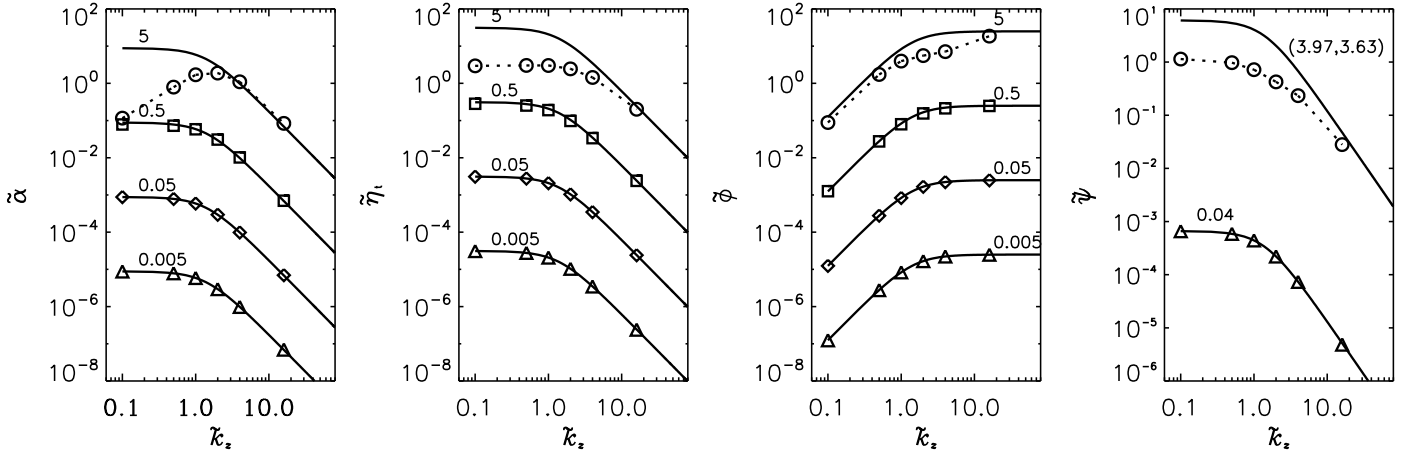


Fig. 4. $\alpha(k_z)$, $\eta_t(k_z)$, and $\phi(k_z)$ for hydromagnetic Roberts forcing with $\text{Pr}_M = 1$ and $\sigma = 1$ (left three panels), likewise $\psi(k_z)$, but for $\sigma = 0.5$ (rightmost panel). Solid lines correspond to SOCA results, cf. Appendix B. Curve labels refer to $\text{Re}_M = \text{Lu}$ or (Re_M, Lu) .

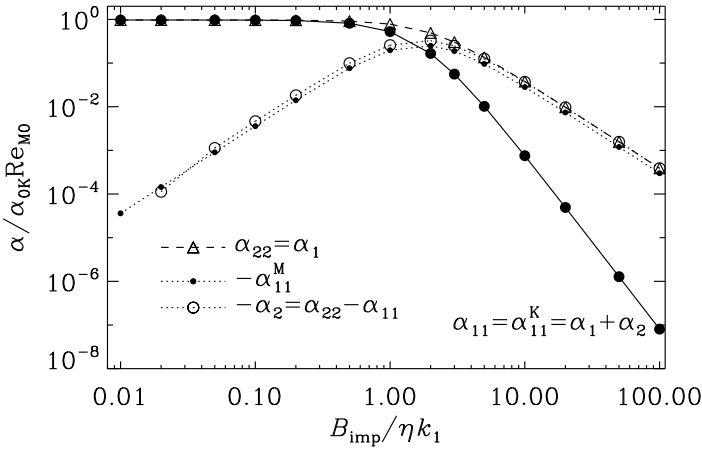


Fig. 5. α_{11} (solid line, filled circles) and α_{22} (dashed line, open triangles) as functions of the imposed field strength B_{imp} , compared with $-\alpha_{11}^M$ (dotted line, small dots) and $\alpha_{22} - \alpha_{11} = -\alpha_2$ (dotted line, open circles) for purely kinetic Roberts forcing with $\tilde{N}_K = 1$ and $\text{Pr}_M = 1$. $\alpha_{11}^M \approx \alpha_2$ throughout. Note that $\alpha_{0K} < 0$ and that the α symbols in the legend refer to the normalized (hence sign-inverted) quantities.

quenching of the effective $\alpha = \alpha_{11}$. Indeed, $\alpha(B_{\text{imp}})$ can be described by a power law with an exponent -4 for large B_{imp} . By comparing with computations in which the non-SOCA term was neglected, we have checked that this discrepancy is not a consequence of SOCA. This is at odds with analytic results predicting either $\alpha \propto B^{-2}$ (Field et al. 1999; Rogachevskii & Kleeorin 2000) or $\propto B^{-3}$ (Moffatt 1972; Rüdiger 1974). Sur et al. (2007) suggested that this difference was due to the fact that the flows are either time-dependent or steady. However, inspecting their Figure 2, their numerical values for α do exhibit the B^{-4} power law. They also found that a α^M , defined similarly to our α_{11} , increases quadratically with \bar{B} for weak fields and declines quadratically for strong fields (Sur et al. 2007). This is in turn in agreement with our present results.

4.2.2. Purely magnetic forcing

Here, the mean electromotive force is simply $\bar{\mathcal{E}} = \bar{\mathcal{E}}_B^M = \overline{\mathbf{u}_B \times \mathbf{b}}$. This is true as long as significant velocities in the main run occur only due to the presence of a mean field, that is, as long as $\mathbf{u}_0 = \mathbf{0}$ (see above). While \bar{B} is weak, $\bar{\mathcal{E}}$ is approximately $\overline{\mathbf{u}_B \times \mathbf{b}_0}$. However, one could speculate that, if the imposed field reaches appreciable levels, i.e., if \mathbf{u} is sufficiently strong, $\bar{\mathcal{E}}$ can, with good accuracy, be approximated by $\bar{\mathcal{E}}_B^K = \overline{\mathbf{u} \times \mathbf{b}_B}$. Since the quasi-kinematic method takes just this term into account, it should then produce useful results.

In Figure 6 we show the rms values of the resulting magnetic and velocity fields as functions of the imposed field strength for $\tilde{N}_M = 1$, corresponding to $\text{Lu} = 1/2$ if $B_{\text{imp}} = 0$. The data points can be fitted by expressions of the form

$$\frac{b_{\text{rms}}}{b_{0\text{rms}}} = \frac{1}{1 + B_{\text{imp}}^2/B_*^2}, \quad \frac{u_{\text{rms}}}{b_{0\text{rms}}} = \frac{B_{\text{imp}}/B_*}{1 + B_{\text{imp}}^2/B_*^2}, \quad (47)$$

where $B_* \approx 1.8 \tilde{N}_M$. Note, that indeed the velocity fluctuations become dominant over the magnetic ones for $B_{\text{imp}}/\eta k_1 > 2$.

The resulting finding, as shown in Figure 7, is completely analogous to the one of Sect. 4.2.1, but now we see $-\alpha_{11}^K \approx -\alpha_2$ approaching $\alpha_{22} = \alpha_1$ with increasing B_{imp} . Hence, the supposition that the quasi-kinematic method could give reasonable results for strong mean fields has not proven true as α_{11}^K is not approaching α_{11} , despite the domination of u_{rms} over b_{rms} . Instead, the values from the quasi-kinematic method have the wrong sign and deviate in their moduli by several orders of magnitude.

In Table 3 we compare, for different values of B_{imp} , the values of α_{11} and α_{22} , obtained using the generalized test-field method, with those of α_{11}^K and those from the quasi-kinematic method, α_{11}^{QK} and α_{22}^{QK} , where the entire dynamics of \mathbf{b}_B has been ignored. Note, again, that the results of all four version of the generalized test-field method agree with each other.

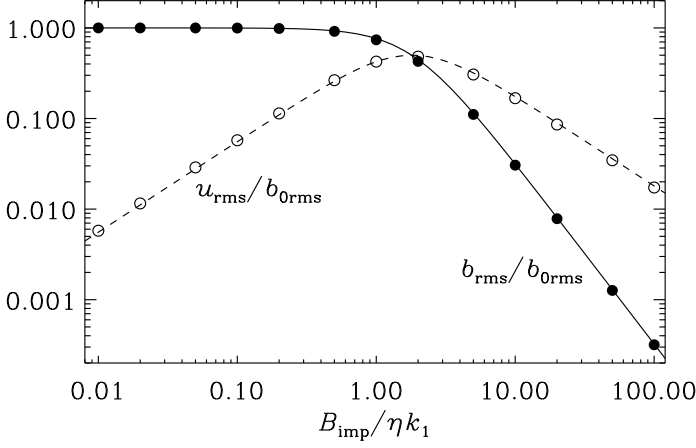


Fig. 6. Root-mean-square values b_{rms} (filled circles) and u_{rms} (open circles) as functions of the imposed field strength B_{imp} for purely magnetic Roberts forcing $\tilde{N}_M = 1$ with $\text{Pr}_M = 1$. The solid and dashed lines represent the fits given by Equation (47).

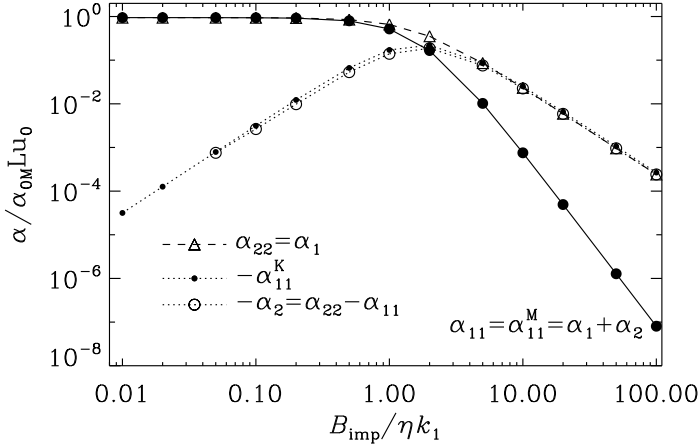


Fig. 7. α_{11} (solid line, filled circles) and α_{22} (dashed line, open triangles) as functions of the imposed field strength B_{imp} , compared with $-\alpha_{11}^K$ (dotted line, small dots) and $\alpha_{22} - \alpha_{11} = -\alpha_2$ (dotted line, open circles) for purely magnetic Roberts forcing with $\tilde{N}_M = 1$ and $\text{Pr}_M = 1$. Note that $\alpha_{11}^K \approx \alpha_2$ throughout.

4.3. Hydromagnetic forcing

Given that the α effect can be sensitive to the value of Pr_M , we study α_{11} and α_{22} as functions of Pr_M , keeping $\text{Lu}/\text{Re}_M = 1$ and $B_{\text{imp}}/\nu k_1 = 1$ fixed. The result is shown in Figure 9.

In the interval $2 \leq \text{Pr}_M \leq 10$ the α coefficients exhibit a high sensitivity with respect to Pr_M changing even their sign at $\text{Pr}_M \approx 0.7$ and 2 , respectively. Note also the occurrence of a minimum and the subsequent growth for $\text{Pr}_M > 4$.

Analogously to Figures 5 and 7 we show in Figure 8 the constituents of α versus B_{imp} . Note that we have used here $\alpha_{0K}\text{Re}_{M0} + \alpha_{0M}\text{Lu}_0 > 0$ for normalizing α which is the kinematic value of $\alpha_{11} = \alpha_{22}$ for $k_z = 0$ and small $u_{0\text{rms}}$, $b_{0\text{rms}}$; see Equations (45) and (46), Sect. 4.1.3.

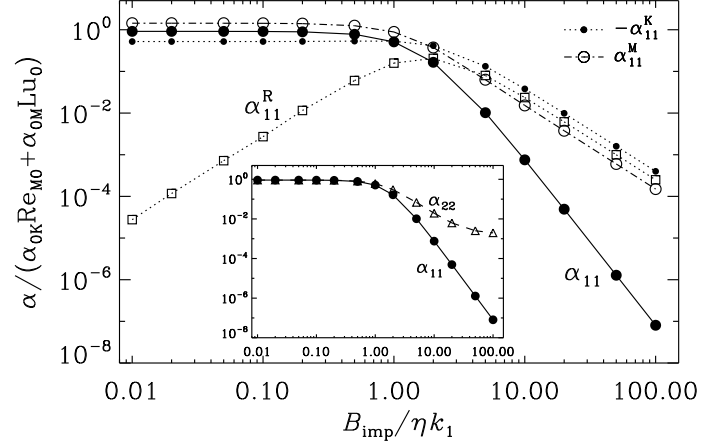


Fig. 8. α_{11} (solid line, filled circles) as function of the imposed field strength B_{imp} , compared with $-\alpha_{11}^K$ (dotted line, small dots), α_{11}^M (dash-dotted line, open circles) and α_{11}^R (dotted line, open squares) for hydromagnetic Roberts forcing with $\tilde{N}_M = \tilde{N}_K = 1$ and $\text{Pr}_M = 1$. The inset shows α_{22} (dashed line, open triangles) compared to α_{11} .

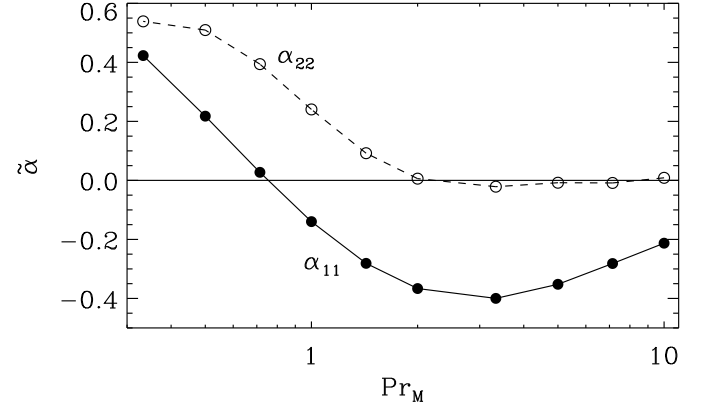


Fig. 9. Dependence of α_{11} and α_{22} on Pr_M for hydromagnetic Roberts forcing with $\text{Lu}/\text{Pr}_M = 1$ and $B_{\text{imp}}/\nu k_1 = 1$.

It can be observed that α_{11}^M at first dominates over $-\alpha_{11}^K$, but at $B_{\text{imp}}/\eta k_1 \approx 10$ their relation reverses. Remarkably, the ratio of the moduli reaches, for high values of B_{imp} , just

Table 3. Dependence of the diagonal components of the α tensor on \tilde{B}_{imp} for $\tilde{N}_M = 1$, $\text{Pr}_M = 1$ using the generalized method ($\tilde{\alpha}_{11}$ and $\tilde{\alpha}_{22}$) together with the kinetic contribution ($\tilde{\alpha}_{11}^K$ and $\tilde{\alpha}_{22}^K$) and the results from the quasi-kinematic method ($\tilde{\alpha}_{11}^{\text{QK}}$ and $\tilde{\alpha}_{22}^{\text{QK}}$).

\tilde{B}_{imp}	10^{-2}	1	10^1	10^2
$\tilde{\alpha}_{11}$	$2.499 \cdot 10^{-1}$	$1.376 \cdot 10^{-1}$	$2.000 \cdot 10^{-4}$	$2.131 \cdot 10^{-8}$
$\tilde{\alpha}_{22}$	$2.499 \cdot 10^{-1}$	$1.747 \cdot 10^{-1}$	$6.161 \cdot 10^{-3}$	$6.390 \cdot 10^{-5}$
$\tilde{\alpha}_{11}^K$	$-8.391 \cdot 10^{-6}$	$-4.540 \cdot 10^{-2}$	$-6.666 \cdot 10^{-3}$	$-7.067 \cdot 10^{-5}$
$\tilde{\alpha}_{11}^{\text{QK}}$	$-7.858 \cdot 10^{-6}$	$-4.350 \cdot 10^{-2}$	$-6.657 \cdot 10^{-3}$	$-7.067 \cdot 10^{-5}$
$\tilde{\alpha}_{22}^{\text{QK}}$	$-2.247 \cdot 10^{-7}$	$-1.152 \cdot 10^{-3}$	$-4.740 \cdot 10^{-7}$	$-5.326 \cdot 10^{-13}$

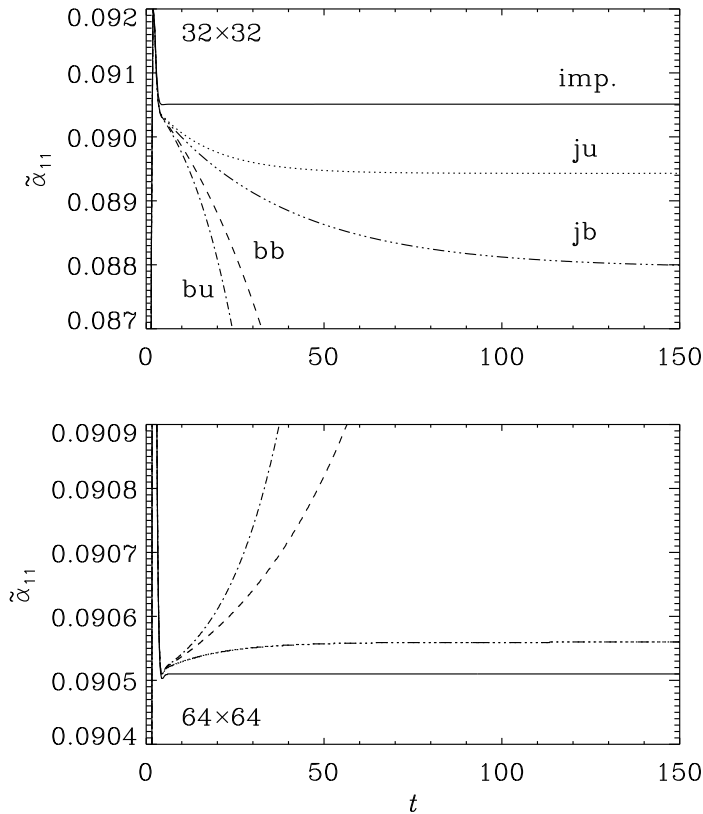


Fig. 10. Convergence of α_{11} the ju and jb versions of the generalized method with the result of the imposed-field method and exponential divergence of the versions bu and bb for $\text{Pr}_M = 1$ with $\tilde{N}_K = \tilde{N}_M = 1$, $\tilde{B}_0 = 1$, $k_z = 0$ and a resolution of either 32^2 mesh points (upper panel) or 64^2 mesh points (lower panel). Note the significant improvement of the converging methods’ agreement by doubling the resolution: The deviation is changing from $\approx 2.5\%$ to $\approx 0.05\%$, that is, by a factor close to 2^6 suggested by the sixth order of the difference scheme.

the inverse of that for low values. The strong quenching of α_{11} is now a consequence of α_{11}^R approaching $-\alpha_{11}^K - \alpha_{11}^M$. In complete agreement with the former two cases with pure forcings, $-\alpha_{11}$ is proportional to B_{imp}^{-4} . However, we see a deviating behavior of $\alpha_{22}(B_{\text{imp}})$ as it is no longer following a power law.

4.4. Convergence

In most of the cases the four different versions of the generalized method, (see Table 1) give quite similar results. For purely hydrodynamic and purely magnetic forcing there is agreement to all significant digits. The agreement becomes somewhat less certain when there is hydromagnetic forcing, i.e. $N_K \neq 0$, $N_M \neq 0$. In general, however, agreement is improved by increasing the numerical resolution.

Yet another complication arises when $B_0 \neq 0$, because then some of the versions display exponentially growing solutions; see Figure 10. We see no other explanation than that by the deliberate rearrangements leading to (34), (35) a potential for spurious instabilities was introduced.

Their real occurrence, however, depends obviously on intricate properties of the fluctuating fields from the main run \mathbf{u} and \mathbf{b} . As the test equations are linear, unlimited exponential growth results (at least for stationary fields in the main runs). We suppose that if one could remove the unstable eigenvalues of the homogeneous version of the system (32)–(35) arbitrarily from its spectrum the solution of the inhomogeneous system would just be the correct one.

5. Discussion

The main purpose of the developed method consists in dealing with situations in which hydrodynamic and magnetic fluctuations coexist. The quasi-kinematic method can only afford those constituents of the mean-field coefficients that are related solely to the hydrodynamic background \mathbf{u}_0 , but the new method is capable of delivering, in addition, those related to the magnetic background \mathbf{b}_0 . Moreover, it is able to detect mean-field effects that depend on cross correlations of \mathbf{u}_0 and \mathbf{b}_0 . We have demonstrated this with the two fluctuations being forced externally to have the same Roberts-like geometry. With respect to α we observe a “magneto-kinetic” part that is, to leading order, quadratic in the magnetic Reynolds and Lundquist numbers and is capable of reducing the total α significantly in comparison with the sum of the α values resulting from purely hydrodynamic and purely magnetic backgrounds. The tensors ϕ and ψ which give rise to the occurrence of mean forces proportional to $\bar{\mathbf{B}}$ (or $\nabla^2 \bar{\mathbf{B}}$) and $\bar{\mathbf{J}}$ are, to leading order, bilinear in Re_M and Lu . In nature, however, external electromotive forces imprinting finite cross-correlations of \mathbf{u}_0 and \mathbf{b}_0 are rarely found. Therefore the question regarding the astrophysical relevance of these effects has to be posed. Given the high values of Re_M in practically all cosmic bodies, small-scale dynamos are supposed to be ubiquitous and do indeed provide hydromagnetic background turbulence. But is it realistic to expect non-vanishing cross-correlations under these circumstances?

Let us consider a number of similar, yet not completely identical turbulence cells arranged in a more or less regular pattern. We assume further that there is some asymmetry between upwellings and downdrafts such that, say, the downdrafts are more efficient in amplifying magnetic fields than the upwellings (Nordlund et al. 1992; Brandenburg et al. 1996). As dynamo fields are solutions of the homogeneous induction equation and the Lorentz force is quadratic in \mathbf{B} , bilinear cross-correlations, $u_{0i}b_{0j}$, obtained by averaging over single cells can be expected to change their sign randomly from cell to cell provided the cellular dynamos have evolved independently from each other. Consequently, the average over many cells would approach zero and the aforementioned effects would not occur. In contrast, cross-correlations that are even functions of the components of \mathbf{b}_0 and their derivatives, were not rendered zero due to polarity changes in the dynamo fields (e.g. the magneto-kinetic α).

However, the assumption of independently acting cellular dynamos can be put in question when the whole process beginning with the onset of the turbulence-creating instability (e.g. convection) is taken into account. During its early stages, i.e. for small magnetic Reynolds numbers, the flow is at first unable to allow for any dynamo action, but with growing amplitude the large-scale dynamo can be excited first to create a field that is coherent over many tur-

bulence cells. With further growth of its amplitude the (hydrodynamic) turbulence eventually enters a stage in which small-scale dynamo action becomes possible. The seed fields for these dynamos are now prevalently determined by the mean field and due to its spatial coherence the polarity of the small-scale field is not settling independently from cell to cell, thus potentially allowing for non-vanishing cross-correlations.

But even if one wants to abstain from employing the influence of a pre-existing mean field it has to be considered that neighboring cells are never exactly equal. Thus, in the course of the growing amplitude of the hydrodynamic background in some of them, the small-scale dynamo will start working first hence setting the seed field for its immediate neighbors. It is well conceivable that the field polarity initiated by one of the early starting cells “cascades” to more and more distant neighbors until this process is limited by the cascades originating from other early starting cells. The result could resemble the domains with uniform field orientation in ferromagnetic materials. Consequently, we arrive at a situation similar to the one discussed before, yet with less extended regions of coinciding field polarity. Instead of employing the idea of a pre-existing large scale dynamo in the cosmic object at hand one may even suppose that, given the smallness of the turbulence cells compared to the scale of the embedding surroundings, there is always a large-scale field, e.g. the galactic one, that is coherent across a large number of turbulence cells.

In summary, cross-correlations and the mean-field effects connected to them are to be considered realistic options. Direct numerical simulations employing the scenarios discussed above should be performed in order to clarify the significance of these effects. This is equally valid for the cross-correlations related effects leading to $\bar{\mathcal{E}}_0$ (see Eq. (29)).

In a recent paper, Courvoisier et al. (2010) discuss the range of applicability of the quasi-kinematic test-field method. Their model consists of the equations of incompressible magneto-hydrodynamics with purely hydrodynamic forcing. However, by imposing an additional uniform magnetic field \mathbf{B} , together with the forced fluctuating velocity a fluctuating magnetic field arises. It must be stressed that, following the further lines of their arguments, these fluctuations have to be considered as part of the *background* ($\mathbf{u}_0, \mathbf{b}_0$), that is, representing just those fluctuations that occur in the *absence* of the mean field. This follows from the fact that, when defining transport coefficients such as α , the field \mathbf{B} is not regarded as part of the mean field $\langle \mathbf{B} \rangle$, in contrast to our treatment; see their section 2.(b). For simplicity they consider only the kinematic case and restrict the analysis to mean fields $\propto e^{ik_z z}$ with $k_z \rightarrow 0$. In their main conclusion, drawn under these conditions, they state that the quasi-kinematic test-field method which considers only the magnetic response to a mean magnetic field must fail for $\mathbf{B} \neq \mathbf{0}$, that is $\mathbf{b}_0 \neq \mathbf{0}$. We fully agree in this respect, but should point out that the method was never claimed to be applicable in that case; see Brandenburg et al. (2008c, Sect. 3), where it is mentioned that “as in almost all supercritical runs a small-scale dynamo is operative, our results which are derived under the assumption of its influence being negligible may contain a systematic error.” However, Courvoisier et al. (2010) overinterpret their finding in postulating that already the determination of

quenched coefficients such as $\alpha(\bar{\mathbf{B}})$ for $\mathbf{b}_0 = \mathbf{0}$ by means of the quasi-kinematic method leads to wrong results. The paper of Tilgner & Brandenburg (2008), quoted by them in this context, is just proving the correctness of the method, as do Brandenburg et al. (2008c).

Our tensor ψ is related to their newly introduced mean-field coefficient Γ by $\psi_{ij} = \epsilon_{kij} \Gamma_{ik}$. Unfortunately, an attempt to reproduce their results for Γ (and likewise for α) is not currently possible owing to our modified hydrodynamics. We postpone this task to a future paper.

6. Conclusions

Having been applied to situations with a magnetohydrodynamic background where both \mathbf{u}_0 and \mathbf{b}_0 have Roberts geometry, the proposed method has proven its potential for determining turbulent transport coefficients. In particular, effects connected with cross-correlations between \mathbf{u}_0 and \mathbf{b}_0 could be identified and are in full agreement with analytical predictions as far as available. No basic restrictions with respect to the magnetic Reynolds number or the strength of the mean field in the main run, which causes the nonlinearity of the problem, are observed so far. As a next step, of course, the simplifications in the hydrodynamics we used will be dropped, thus allowing to produce more relevant results and facilitating comparisons with work already done.

Due to the fact that we have no strict mathematical proof for its correctness, there can be no full certainty about the general reliability of the method. As a hopeful indication, in many cases, all four flavors of the method produce practically identical results, but occasionally some of them show, for unknown reasons, unstable behavior in the test solutions. Clearly, further exploration of the method’s degree of reliance by including three-dimensional and time-dependent backgrounds is necessary. Homogeneity should be abandoned and backgrounds which come closer to real turbulence such as forced turbulence or turbulent convection in a layer are to be taken into account.

Thus, the utilized approach of establishing a test-field procedure in a situation where the governing equations are inherently nonlinear, although by virtue of the Lorentz force only, has proven to be promising. This fact encourages us to develop test-field methods for determining turbulent transport coefficients connected with similar nonlinearities in the momentum equation. An interesting target is the turbulent kinematic viscosity tensor, and especially its off-diagonal components that can give rise to a mean-field vorticity dynamo (Elperin et al. 2007; Käpylä et al. 2009), as well as the so-called anisotropic kinematic α effect (Frisch et al. 1987; Sulem et al. 1989; Brandenburg & von Rekowski 2001; Courvoisier et al. 2010) and the Λ effect (Rüdiger 1980, 1982). Yet another example is given by the turbulent transport coefficients describing effective magnetic pressure and tension forces due to the quadratic dependence of the total Reynolds stress tensor on the mean magnetic field (e.g., Rogachevskii & Kleeorin 2007; Brandenburg et al. 2010).

Appendix A: Incompressibility

The equations used in this paper had the advantage of simplifying the derivation of the generalized test-field method, but the resulting flows are not realistic because the pressure

and advective terms are absent. Here we drop these restrictions and derive the test equations in the incompressible case with constant density. The full momentum and induction equations take then the form

$$\frac{\partial \mathbf{U}}{\partial t} = \mathbf{U} \times \mathbf{W} + \mathbf{J} \times \mathbf{B} + \mathbf{F}_K + \nu \nabla^2 \mathbf{U} - \nabla P, \quad (\text{A.1})$$

$$\frac{\partial \mathbf{A}}{\partial t} = \mathbf{U} \times \mathbf{B} + \mathbf{F}_M + \eta \nabla^2 \mathbf{A}. \quad (\text{A.2})$$

where $\mathbf{W} = \text{curl} \mathbf{U}$ is the vorticity and P is the sum of gas and dynamical pressure and absorbs the constant density. The corresponding mean-field equations are

$$\frac{\partial \overline{\mathbf{U}}}{\partial t} = \overline{\mathbf{U}} \times \overline{\mathbf{W}} + \overline{\mathbf{J}} \times \overline{\mathbf{B}} + \overline{\mathcal{F}} + \nu \nabla^2 \overline{\mathbf{U}} - \nabla \overline{P}, \quad (\text{A.3})$$

$$\frac{\partial \overline{\mathbf{A}}}{\partial t} = \overline{\mathbf{U}} \times \overline{\mathbf{B}} + \overline{\mathcal{E}} + \eta \nabla^2 \overline{\mathbf{A}}, \quad (\text{A.4})$$

where $\overline{\mathcal{F}} = \overline{\mathbf{u} \times \mathbf{w}} + \overline{\mathbf{j} \times \mathbf{b}}$ and $\overline{\mathcal{E}} = \overline{\mathbf{u} \times \mathbf{b}}$, and the forcings were assumed to vanish on averaging. The equations for the fluctuations are consequently

$$\begin{aligned} \frac{\partial \mathbf{u}}{\partial t} = & \overline{\mathbf{U}} \times \mathbf{w} + \mathbf{u} \times \overline{\mathbf{W}} + \overline{\mathbf{J}} \times \mathbf{b} + \mathbf{j} \times \overline{\mathbf{B}} \\ & + \mathcal{F}' + \mathbf{F}_K + \nu \nabla^2 \mathbf{u} - \nabla p, \end{aligned} \quad (\text{A.5})$$

$$\frac{\partial \mathbf{a}}{\partial t} = \overline{\mathbf{U}} \times \mathbf{b} + \mathbf{u} \times \overline{\mathbf{B}} + \mathcal{E}' + \mathbf{F}_M + \eta \nabla^2 \mathbf{a}, \quad (\text{A.6})$$

where $\mathcal{F}' = (\mathbf{u} \times \mathbf{w} + \mathbf{j} \times \mathbf{b})'$ and $\mathcal{E}' = (\mathbf{u} \times \mathbf{b})'$. As above we split the fields and likewise the Equations (A.5) and (A.6) into two parts, i.e. we write $\mathbf{u} = \mathbf{u}_0 + \mathbf{u}_{\overline{\mathbf{B}}}$ and $\mathbf{a} = \mathbf{a}_0 + \mathbf{a}_{\overline{\mathbf{B}}}$ and arrive at

$$\frac{\partial \mathbf{u}_0}{\partial t} = \overline{\mathbf{U}} \times \mathbf{w}_0 + \mathbf{u}_0 \times \overline{\mathbf{W}} + \mathcal{F}'_0 + \mathbf{F}_K + \nu \nabla^2 \mathbf{u}_0 - \nabla p_0, \quad (\text{A.7})$$

$$\frac{\partial \mathbf{a}_0}{\partial t} = \overline{\mathbf{U}} \times \mathbf{b}_0 + \mathcal{E}'_0 + \mathbf{F}_M + \eta \nabla^2 \mathbf{a}_0, \quad (\text{A.8})$$

and the equations for the $\overline{\mathbf{B}}$ dependent parts

$$\begin{aligned} \frac{\partial \mathbf{u}_{\overline{\mathbf{B}}}}{\partial t} = & \overline{\mathbf{U}} \times \mathbf{w}_{\overline{\mathbf{B}}} + \mathbf{u}_{\overline{\mathbf{B}}} \times \overline{\mathbf{W}} + \overline{\mathbf{J}} \times \mathbf{b} + \mathbf{j} \times \overline{\mathbf{B}} \\ & + \mathcal{F}'_{\overline{\mathbf{B}}} + \nu \nabla^2 \mathbf{u}_{\overline{\mathbf{B}}} - \nabla p_{\overline{\mathbf{B}}} \end{aligned} \quad (\text{A.9})$$

$$\frac{\partial \mathbf{a}_{\overline{\mathbf{B}}}}{\partial t} = \overline{\mathbf{U}} \times \mathbf{b}_{\overline{\mathbf{B}}} + \mathbf{u}_{\overline{\mathbf{B}}} \times \overline{\mathbf{B}} + \mathcal{E}'_{\overline{\mathbf{B}}} + \eta \nabla^2 \mathbf{a}_{\overline{\mathbf{B}}}, \quad (\text{A.10})$$

where $\mathcal{F}' = \mathcal{F}'_0 + \mathcal{F}'_{\overline{\mathbf{B}}}$ and $\mathcal{E}' = \mathcal{E}'_0 + \mathcal{E}'_{\overline{\mathbf{B}}}$ with $\mathcal{F}'_0 = (\mathbf{u}_0 \times \mathbf{w}_0 + \mathbf{j}_0 \times \mathbf{b}_0)'$, $\mathcal{E}'_0 = (\mathbf{u}_0 \times \mathbf{b}_0)'$, and

$$\begin{aligned} \mathcal{F}'_{\overline{\mathbf{B}}} = & (\mathbf{j}_0 \times \mathbf{b}_{\overline{\mathbf{B}}} + \mathbf{j}_{\overline{\mathbf{B}}} \times \mathbf{b}_0 + \mathbf{j}_{\overline{\mathbf{B}}} \times \mathbf{b}_{\overline{\mathbf{B}}} \\ & + \mathbf{u}_0 \times \mathbf{w}_{\overline{\mathbf{B}}} + \mathbf{u}_{\overline{\mathbf{B}}} \times \mathbf{w}_0 + \mathbf{u}_{\overline{\mathbf{B}}} \times \mathbf{w}_{\overline{\mathbf{B}}})', \end{aligned} \quad (\text{A.11})$$

$$\mathcal{E}'_{\overline{\mathbf{B}}} = (\mathbf{u}_0 \times \mathbf{b}_{\overline{\mathbf{B}}} + \mathbf{u}_{\overline{\mathbf{B}}} \times \mathbf{b}_0 + \mathbf{u}_{\overline{\mathbf{B}}} \times \mathbf{b}_{\overline{\mathbf{B}}})'. \quad (\text{A.12})$$

We can rewrite these equations such that they become formally linear in $\mathbf{u}_{\overline{\mathbf{B}}}$ and $\mathbf{b}_{\overline{\mathbf{B}}}$. Following the pattern utilized in Sect. 3.3 we find already for $\mathcal{F}'_{\overline{\mathbf{B}}}$ four different ways of doing that. Together with the two variants in the case of $\mathcal{E}'_{\overline{\mathbf{B}}}$ we finally obtain eight flavors of the test-field method where again in either case $\overline{\mathcal{F}}$ and $\overline{\mathcal{E}}$ are to be constructed

analogously to $\mathcal{F}'_{\overline{\mathbf{B}}}$ and $\mathcal{E}'_{\overline{\mathbf{B}}}$. One of these flavors is defined by

$$\mathcal{F}'_{\overline{\mathbf{B}}} = (\mathbf{u} \times \mathbf{w}_{\overline{\mathbf{B}}} + \mathbf{u}_{\overline{\mathbf{B}}} \times \mathbf{w}_0 + \mathbf{j} \times \mathbf{b}_{\overline{\mathbf{B}}} + \mathbf{j}_{\overline{\mathbf{B}}} \times \mathbf{b}_0)', \quad (\text{A.13})$$

$$\mathcal{E}'_{\overline{\mathbf{B}}} = (\mathbf{u} \times \mathbf{b}_{\overline{\mathbf{B}}} + \mathbf{u}_{\overline{\mathbf{B}}} \times \mathbf{b}_0)'. \quad (\text{A.14})$$

It is the one which comes closest to the quasi-kinematic test-field method, because there $\mathcal{E}'_{\overline{\mathbf{B}}} = (\mathbf{u} \times \mathbf{b}_{\overline{\mathbf{B}}})'$. Next, we substitute $\overline{\mathbf{B}}$ by a test field, $\overline{\mathbf{B}}^T$, and $\mathbf{u}_{\overline{\mathbf{B}}}$ and $\mathbf{b}_{\overline{\mathbf{B}}}$ by the test solutions, \mathbf{u}^T and \mathbf{b}^T , i.e.

$$\begin{aligned} \frac{\partial \mathbf{u}^T}{\partial t} = & \overline{\mathbf{U}} \times \mathbf{w}^T + \mathbf{u}^T \times \overline{\mathbf{W}} + \overline{\mathbf{J}}^T \times \mathbf{b} + \mathbf{j} \times \overline{\mathbf{B}}^T \\ & + \mathcal{F}'_T + \nu \nabla^2 \mathbf{u}^T - \nabla p^T, \end{aligned} \quad (\text{A.15})$$

$$\frac{\partial \mathbf{a}^T}{\partial t} = \overline{\mathbf{U}} \times \mathbf{b}^T + \mathbf{u} \times \overline{\mathbf{B}}^T + \mathcal{E}'_T + \eta \nabla^2 \mathbf{a}^T, \quad (\text{A.16})$$

where

$$\mathcal{F}'_T = (\mathbf{u} \times \mathbf{w}^T + \mathbf{u}^T \times \mathbf{w}_0 + \mathbf{j} \times \mathbf{b}^T + \mathbf{j}^T \times \mathbf{b}_0)', \quad (\text{A.17})$$

$$\mathcal{E}'_T = (\mathbf{u} \times \mathbf{b}^T + \mathbf{u}^T \times \mathbf{b}_0)'. \quad (\text{A.18})$$

For the mean electromotive force and force the ansatzes (8) and (16) can be employed without change. Note, however, that the tensors ϕ and ψ now contain contributions from the Reynolds stress created by $\mathbf{u}_{\overline{\mathbf{B}}}$, that is eventually, by $\overline{\mathbf{B}}$. From the point of view of the tensorial structure of the relationship between $\overline{\mathbf{B}}$ and $\overline{\mathcal{F}}$ or $\overline{\mathcal{E}}$ the ansatzes (8) and (16) provide full generality as long as only the mean field and its first spatial derivative are to be included. That's why there are no separate terms with the mean velocity or its gradient tensor. Instead the latter play the role of problem parameters and all transport coefficients can of course be determined as functions of them. A separate task would consist in determining the tensors which appear in an analogous form of (29) in place of the scalar coefficients when a general anisotropic background is given. Then a test method with respect to $\overline{\mathbf{U}}$ had to be tailored.

Appendix B: Derivation of $\phi(k_z)$, $\psi(k_z)$

Start with the stationary induction equation in SOCA

$$\eta \nabla^2 \mathbf{b}_{\overline{\mathbf{B}}} + \text{curl}(\mathbf{u}_0 \times \overline{\mathbf{B}}) = \mathbf{0}. \quad (\text{B.1})$$

Assume $\mathbf{u}_0 = u_{0\text{rms}} \mathbf{f}$ and $\mathbf{b}_0 = b_{0\text{rms}} \mathbf{f}$ with $\mathbf{f} = \mathbf{f}(x, y)$, $\text{curl} \mathbf{f} = k_f \mathbf{f}$, $\overline{\mathbf{f}^2} = 1$, $\overline{\mathbf{B}} = \hat{\mathbf{B}} e^{ik_z z}$, and $\hat{B}_{x,y} = \text{const}$, $\hat{B}_z = 0$. Hence $\nabla^2 \mathbf{f} = -k_f^2 \mathbf{f}$. Then we can make the ansatz $\mathbf{b}_{\overline{\mathbf{B}}} = \hat{\mathbf{b}}(x, y) e^{ik_z z}$ with $\nabla^2 \hat{\mathbf{b}} = -k_f^2 \hat{\mathbf{b}}$ and get

$$\mathbf{b}_{\overline{\mathbf{B}}} = \frac{1}{\eta} \frac{1}{k_f^2 + k_z^2} ((\overline{\mathbf{B}} \cdot \nabla) \mathbf{u}_0 - ik_z u_{0z} \overline{\mathbf{B}})$$

For the calculation of the mean force

$$\overline{\mathcal{F}}_{\overline{\mathbf{B}}} = \overline{\mathbf{j}_0 \times \mathbf{b}_{\overline{\mathbf{B}}} + \mathbf{j}_{\overline{\mathbf{B}}} \times \mathbf{b}_0}$$

we need further

$$\mathbf{j}_{\overline{\mathbf{B}}} = \text{curl} \mathbf{b}_{\overline{\mathbf{B}}} = \text{curl}(e^{ik_z z} \hat{\mathbf{b}}) = e^{ik_z z} (\text{curl} \hat{\mathbf{b}} + ik_z \hat{\mathbf{z}} \times \hat{\mathbf{b}}) \quad (\text{B.2})$$

$$= \frac{k_f}{\eta(k_f^2 + k_z^2)} ((\overline{\mathbf{B}} \cdot \nabla) \mathbf{u}_0 + ik_z (\overline{\mathbf{B}} \cdot \mathbf{u}_0) \hat{\mathbf{z}}) + ik_z \hat{\mathbf{z}} \times \mathbf{b}_{\overline{\mathbf{B}}}. \quad (\text{B.3})$$

Consequently

$$\begin{aligned}\overline{\mathcal{F}}_{\overline{\mathbf{B}}} &= k_f \overline{\mathbf{b}_0} \times \overline{\mathbf{b}_{\overline{\mathbf{B}}}} + \overline{\mathbf{j}_{\overline{\mathbf{B}}}} \times \overline{\mathbf{b}_0} \\ &= \frac{1}{\eta} \frac{1}{k_f^2 + k_z^2} \left(\overline{ik_z (k_f (\overline{\mathbf{B}} \cdot \mathbf{u}_0) \hat{\mathbf{z}} + k_f u_{0z} \overline{\mathbf{B}} + \hat{\mathbf{z}} \times (\overline{\mathbf{B}} \cdot \nabla) \mathbf{u}_0) \times \mathbf{b}_0} \right. \\ &\quad \left. + k_z^2 \overline{u_{0z} (\hat{\mathbf{z}} \times \overline{\mathbf{B}}) \times \mathbf{b}_0} \right) \\ &= \frac{1}{\eta} \frac{1}{k_f^2 + k_z^2} \left(\overline{ik_z k_f ((\overline{\mathbf{B}} \cdot \mathbf{u}_0) \hat{\mathbf{z}} + u_{0z} \overline{\mathbf{B}}) \times \mathbf{b}_0} \right. \\ &\quad \left. + \overline{ik_z b_{0z} (\overline{\mathbf{B}} \cdot \nabla) \mathbf{u}_0 - \hat{\mathbf{z}} \mathbf{b}_0 \cdot (\overline{\mathbf{B}} \cdot \nabla) \mathbf{u}_0} \right. \\ &\quad \left. + k_z^2 (\overline{u_{0z} b_{0z} \overline{\mathbf{B}} - \hat{\mathbf{z}} \overline{u_{0z} \mathbf{b}_0} \cdot \overline{\mathbf{B}}) \right)\end{aligned}$$

and with $\overline{\mathbf{J}} = ik_z \hat{\mathbf{z}} \times \overline{\mathbf{B}}$, that is, $ik_z B_k = \epsilon_{k i 3} \overline{J}_i$, $k = 1, 2$,

$$\begin{aligned}\overline{\mathcal{F}}_{\overline{\mathbf{B}} i} &= \frac{1}{\eta} \frac{1}{k_f^2 + k_z^2} \left(k_f (\epsilon_{i 3 k} \epsilon_{m l 3} \overline{u_{0m} b_{0k}} - \epsilon_{i j k} \epsilon_{k l 3} \overline{u_{0z} b_{0j}}) \overline{J}_l \right. \\ &\quad \left. + \epsilon_{l j 3} \left(-\overline{b_{0z} \frac{\partial u_{0i}}{\partial x_j}} + \delta_{i 3} \overline{\mathbf{b}_0} \cdot \frac{\partial \mathbf{u}_0}{\partial x_j} \right) \overline{J}_l \right. \\ &\quad \left. + k_z^2 (\overline{u_{0z} b_{0z} \overline{B}_i} - \delta_{i 3} \overline{u_{0z} b_{0l} \overline{B}_l}) \right).\end{aligned}$$

The tensors are hence

$$\begin{aligned}\phi_{il} &= \frac{1}{\eta} \frac{k_z^2}{k_f^2 + k_z^2} (\overline{u_{0z} b_{0z} \delta_{il}} - \overline{u_{0z} b_{0l} \delta_{i 3}}), \\ \psi_{il} &= \frac{1}{\eta} \frac{1}{k_f^2 + k_z^2} \left(k_f (\overline{u_{0z} b_{0z} \delta_{il}} - \overline{u_{0z} b_{0l} \delta_{i 3}}) \right. \\ &\quad \left. + k_f (1 - \delta_{i 3}) (\overline{u_{0i} b_{0l}} - \delta_{il} (\overline{u_{01} b_{01}} + \overline{u_{02} b_{02}})) \right. \\ &\quad \left. + \epsilon_{l j 3} \left(\overline{b_{0z} \frac{\partial u_{0i}}{\partial x_j}} - \overline{\mathbf{b}_0} \cdot \frac{\partial \mathbf{u}_0}{\partial x_j} \delta_{i 3} \right) \right), \quad l \neq 3 \\ \phi_{i 3} &= \psi_{i 3} = 0.\end{aligned}$$

For $k_z \rightarrow 0$ the tensor ϕ is proportional to k_z^2 thus the corresponding mean force expressed in physical space by a convolution $\check{\phi} \circ \overline{\mathbf{B}}$, with $\check{\phi}$ being the Fourier-backtransformed ϕ , can be approximated by a term $\propto \partial^2 \overline{\mathbf{B}} / \partial z^2$. For $k_z \gg k_f$, however, the mean force can be represented by a term $\propto \overline{\mathbf{B}}$.

With Roberts geometry we have for $\sigma = 1$

$$\phi_{11} = \phi_{22} = \frac{1}{2\eta} \frac{k_z^2}{k_f^2 + k_z^2} u_{0\text{rms}} b_{0\text{rms}}, \quad \psi = \mathbf{0}.$$

All other ϕ components vanish, too.

If, however, for the Roberts geometry $0 \leq \sigma < 1$ the field \mathbf{f} has indeed yet the property $\nabla^2 \mathbf{f} = -k_f^2 \mathbf{f}$, but is no longer of Beltrami type. Instead, we have

$$\text{curl } \mathbf{f} = \sigma k_f (\mathbf{f} + \frac{1 - \sigma^2}{\sigma^2} f_z \hat{\mathbf{z}}).$$

The tensor ψ does not vanish any longer, but is now given by

$$\begin{aligned}\psi_{11} &= -\frac{1}{\eta(k_f^2 + k_z^2)} \frac{k_y^2(1 - \sigma^2)}{k_f(1 + \sigma^2)} u_{0\text{rms}} b_{0\text{rms}}, \\ \psi_{22} &= -\frac{1}{\eta(k_f^2 + k_z^2)} \frac{k_x^2(1 - \sigma^2)}{k_f(1 + \sigma^2)} u_{0\text{rms}} b_{0\text{rms}}, \\ \psi_{12} &= \psi_{21} = 0.\end{aligned}$$

Appendix C: Illustration of extracting a linear evolution equation from a nonlinear one

To illustrate the procedure of extracting a linear evolution equation from a nonlinear problem, let us consider a simple quadratic ordinary differential equation, $y' = y^2$, where a prime denotes here differentiation. We split y into two parts, $y = y_N + y_L$, so we have

$$y^2 = y_N^2 + 2y_N y_L + y_L^2. \quad (\text{C.1})$$

In the last two terms we can replace $y_N + y_L$ by y , so we have $2y_N y_L + y_L^2 = (y_N + y) y_L$, which is now formally linear in y_L . Here, y corresponds to the solution of the ‘main run’. Thus, at the expense of having to solve an additional nonlinear auxiliary equation, $y'_N = y_N^2$, we have extracted a linear evolution equation for y_L . Altogether we have

$$\begin{cases} y' = y^2, \\ y'_N = y_N^2, \\ y'_L = (y_N + y) y_L, \end{cases} \quad (\text{C.2})$$

where the last equation is linear in y_L . Note, that the system (C.2) is exactly equivalent to (C.1), i.e. no approximation has been made.

Appendix D: Derivation of (46)

Consider the stationary version of (22) with $\mathcal{F}'_{\overline{\mathbf{B}}}$ dropped (i.e. SOCA) and a uniform $\overline{\mathbf{B}}$, i.e., $\overline{\mathbf{J}} = \mathbf{0}$

$$\nu \nabla^2 \mathbf{u}_{\overline{\mathbf{B}}} + \mathbf{j} \times \overline{\mathbf{B}} = \mathbf{0}. \quad (\text{D.1})$$

Assume $\mathbf{b} = \text{curl } \mathbf{a}$, $\text{div } \mathbf{a} = 0$, hence $\mathbf{j} = -\nabla^2 \mathbf{a}$. We get

$$\mathbf{u}_{\overline{\mathbf{B}}} = \mathbf{a} \times \overline{\mathbf{B}} / \nu \quad (\text{D.2})$$

and further

$$(\overline{\mathbf{u}_{\overline{\mathbf{B}}} \times \mathbf{b}})_i = \frac{1}{\nu} \epsilon_{ilm} \epsilon_{lkj} \overline{a_k b_m} \overline{B}_j = \alpha_{ij} \overline{B}_j$$

that is,

$$\alpha_{ij} = (\overline{\mathbf{a} \cdot \mathbf{b}} \delta_{ij} - \overline{a_i b_j}) / \nu.$$

Isotropy results in

$$\alpha = \alpha_{ii} / 3 = 2 \overline{\mathbf{a} \cdot \mathbf{b}} / 3\nu.$$

For \mathbf{b} with Roberts geometry, however, we have $\alpha = \alpha_{11} = \alpha_{22} \neq \alpha_{33}$, hence

$$\alpha = (\overline{\mathbf{a} \cdot \mathbf{b}} + \overline{a_3 b_3}) / 2\nu = k_f (\overline{\mathbf{a}^2} + \overline{a_3^2}) / 2\nu = 3b_{\text{rms}}^2 / 4k_f \nu$$

and with $\text{Lu} = b_{\text{rms}} / \eta k_f$

$$\alpha = \frac{3}{4} b_{\text{rms}} \text{Lu} / \text{Pr}_M. \quad (\text{D.3})$$

Adopt now a $\overline{\mathbf{B}}$ depending on z only with $\overline{\mathbf{B}} \propto e^{ik_z z}$, but \mathbf{b} , \mathbf{a} still independent of z . Roberts geometry implies $\nabla^2 \mathbf{a} = -k_f^2 \mathbf{a}$ and $\nabla^2 \mathbf{u}_{\overline{\mathbf{B}}} = -(k_f^2 + k_z^2) \mathbf{u}_{\overline{\mathbf{B}}}$. Inserting in (D.1) (with the term proportional to $\overline{\mathbf{J}}$ omitted) yields

$$(k_f^2 + k_z^2) \mathbf{u}_{\overline{\mathbf{B}}} = k_f^2 \mathbf{a} \times \overline{\mathbf{B}} / \nu + \dots$$

and comparison with (D.2) reveals that (D.3) has only to be modified by the factor $1 / (1 + (k_z / k_f)^2)$.

Appendix E: Derivation of α_{mk} in fourth order approximation

We employ the iterative procedure described, e.g., in Rädler & Rheinhardt (2007) to obtain those contributions to $\bar{\mathcal{E}}_{\bar{B}}$ which are quadratic in $u_{0\text{rms}}$ and $b_{0\text{rms}}$ and expand for that purpose $\mathbf{b}_{\bar{B}}$ and $\mathbf{u}_{\bar{B}}$ into the series

$$\begin{aligned}\mathbf{b}_{\bar{B}} &= \mathbf{b}_{\bar{B}}^{(1)} + \mathbf{b}_{\bar{B}}^{(2)} + \mathbf{b}_{\bar{B}}^{(3)} + \dots, \\ \mathbf{u}_{\bar{B}} &= \mathbf{u}_{\bar{B}}^{(1)} + \mathbf{u}_{\bar{B}}^{(2)} + \mathbf{u}_{\bar{B}}^{(3)} + \dots\end{aligned}$$

with

$$\begin{aligned}\eta \nabla^2 \mathbf{b}_{\bar{B}}^{(1)} &= -\text{curl}(\mathbf{u}_0 \times \bar{\mathbf{B}}) \\ \nu \nabla^2 \mathbf{u}_{\bar{B}}^{(1)} &= -(\mathbf{j}_0 \times \bar{\mathbf{B}} + \bar{\mathbf{J}} \times \mathbf{b}_0) \\ \eta \nabla^2 \mathbf{b}_{\bar{B}}^{(i)} &= -\text{curl}(\mathbf{u}_0 \times \mathbf{b}_{\bar{B}}^{(i-1)} + \mathbf{u}_{\bar{B}}^{(i-1)} \times \mathbf{b}_0) \\ \nu \nabla^2 \mathbf{u}_{\bar{B}}^{(i)} &= -(\mathbf{j}_0 \times \mathbf{b}_{\bar{B}}^{(i-1)} + \mathbf{j}_{\bar{B}}^{(i-1)} \times \mathbf{b}_0), \quad i = 2, \dots\end{aligned}$$

and

$$\bar{\mathcal{E}}_{\bar{B}} = \sum_{i=1}^{\infty} \left(\overline{\mathbf{u}_0 \times \mathbf{b}_{\bar{B}}^{(i)}} + \overline{\mathbf{u}_{\bar{B}}^{(i)} \times \mathbf{b}_0} \right) = \sum_{i=1}^{\infty} \bar{\mathcal{E}}_{\bar{B}}^{(i)}$$

In the following we assume $\bar{\mathbf{B}}$ to be uniform and $\mathbf{u}_0, \mathbf{b}_0$ to have Roberts geometry (43). The SOCA solutions $\mathbf{b}_{\bar{B}}^{(1)}$ and $\mathbf{u}_{\bar{B}}^{(1)}$ read

$$\mathbf{b}_{\bar{B}}^{(1)} = \frac{1}{\eta k_f^2} (\bar{\mathbf{B}} \cdot \nabla) \mathbf{u}_0, \quad \mathbf{u}_{\bar{B}}^{(1)} = \frac{1}{\nu k_f} \mathbf{b}_0 \times \bar{\mathbf{B}}.$$

From here on we switch to dimensionless quantities and set $\eta = \nu = 1, k_x = k_y = 1, k_f = \sqrt{2}, |\bar{\mathbf{B}}| = 1$. So we have

$$\begin{aligned}\mathbf{b}_{\bar{B}}^{(1)} &= \frac{u_{0\text{rms}}}{2} [\sin x \sin y, \cos x \cos y, -\sqrt{2} \sin x \cos y] \\ \mathbf{u}_{\bar{B}}^{(1)} &= \frac{b_{0\text{rms}}}{2} [0, 2 \cos x \cos y, -\sqrt{2} \sin x \cos y] \\ \mathbf{u}_{\bar{B}}^{(2)} &= \mathbf{0} \\ \mathbf{b}_{\bar{B}}^{(2)} &= \frac{1}{8} \left(-u_{0\text{rms}}^2 [\cos 2y, 0, \sqrt{2} \sin 2y] + \frac{b_{0\text{rms}}^2}{2} \right. \\ &\quad \left. [\cos 2y(\cos 2x + 2), \sin 2y \sin 2x, \sqrt{2} \sin 2y(\cos 2x + 3)] \right).\end{aligned}$$

For $\mathbf{b}_{\bar{B}}^{(3)}$ and $\mathbf{u}_{\bar{B}}^{(3)}$ we present here only those parts which eventually contribute to α_{mk} :

$$\begin{aligned}\mathbf{b}_{\bar{B}}^{(3)} &= \frac{u_{0\text{rms}} b_{0\text{rms}}^2}{32} [\sin x \sin y, \cos x \cos y, -4\sqrt{2} \sin x \cos y] \\ &\quad + \dots \\ \mathbf{u}_{\bar{B}}^{(3)} &= \frac{u_{0\text{rms}}^2 b_{0\text{rms}}}{16} [0, \cos x \cos y, -\frac{\sqrt{2}}{2} \sin x \cos y] + \dots\end{aligned}$$

Finally,

$$\bar{\mathcal{E}}_{\bar{B}}^{(3)} = \overline{\mathbf{u}_0 \times \mathbf{b}_{\bar{B}}^{(3)}} + \overline{\mathbf{u}_{\bar{B}}^{(3)} \times \mathbf{b}_0} = -u_{0\text{rms}}^2 b_{0\text{rms}}^2 \frac{\sqrt{2}}{64} + \dots,$$

i.e.

$$\alpha_{\text{mk}} \approx -u_{0\text{rms}}^2 b_{0\text{rms}}^2 \frac{\sqrt{2}}{64}.$$

Note, that the contributions omitted in $\bar{\mathcal{E}}_{\bar{B}}^{(3)}$ provide fourth order corrections to α_k and α_m . They result in dependences on Re_M and Lu that are weaker than the parabolic SOCA ones; see Fig. 3.

References

- Beck, R., Poezd, A. D., Shukurov, A., Sokoloff, D. D. 1994, A&A, 289, 94
- Beck, R., Brandenburg, A., Moss, D., Shukurov, A., & Sokoloff, D. 1996, ARA&A, 34, 155
- Brandenburg, A. 2001, ApJ, 550, 824
- Brandenburg, A. 2005a, ApJ, 625, 539
- Brandenburg, A. 2005b, Astron. Nachr., 326, 787
- Brandenburg, A., & Käpylä, P. J. 2007, New J. Phys., 9, 305, 1
- Brandenburg, A., & Subramanian, K. 2005, Phys. Rep. 417, 1
- Brandenburg, A., & von Rekowski, B. 2001, A&A, 379, 1153
- Brandenburg, A., Jennings, R. L., Nordlund, Å., Rieutord, M., Stein, R. F., & Tuominen, I. 1996, J. Fluid Mech., 306, 325
- Brandenburg, A., Dobler, W., & Subramanian, K. 2002, Astron. Nachr., 323, 99
- Brandenburg, A., Kleeorin, N., & Rogachevskii, I. 2010, Astron. Nachr., 331, 5
- Brandenburg, A., Rädler, K.-H., & Schrunner, M. 2008a, A&A, 482, 739
- Brandenburg, A., Rädler, K.-H., Rheinhardt, M., & Käpylä, P. J. 2008b, ApJ, 676, 740
- Brandenburg, A., Rädler, K.-H., Rheinhardt, M., & Subramanian, K. 2008c, ApJ, 687, L49
- Cattaneo, F. 1999, ApJ, 515, L39
- Cho, J., & Vishniac, E. 2000, ApJ, 538, 217
- Courvoisier A., Hughes D. W., Proctor M. R. E. 2010, Proc. Roy. Soc. Lond., 466, 583
- Elperin, T., Golubev, I., Kleeorin, N., & Rogachevskii, I. 2007, Phys. Rev. E, 76, 066310
- Emonet, T., & Cattaneo, F. 2001, ApJ, 560, L197
- Field, G. B., Blackman, E. G., & Chou H. 1999, ApJ, 513, 638
- Frisch, U., She, Z. S., & Sulem, P. L. 1987, Physica, 28D, 382
- Haugen, N. E. L., Brandenburg, A., & Dobler, W. 2003, ApJ, 597, L141
- Haugen, N. E. L., Brandenburg, A., & Dobler, W. 2004, Phys. Rev. E, 70, 016308
- Hubbard, A., & Brandenburg, A. 2009, ApJ, 706, 712
- Käpylä, P. J., Korpi, M. J., & Brandenburg, A. 2008, A&A, 491, 353
- Käpylä, P. J., Mitra, D., & Brandenburg, A. 2009, Phys. Rev. E, 79, 016302
- Kazantsev, A. P. 1968, Sov. Phys. JETP, 26, 1031
- Krause, F., & Rädler, K.-H. 1980, Mean-field magnetohydrodynamics and dynamo theory (Pergamon Press, Oxford)
- Mitra, D., Käpylä, P. J., Tavakol, R., & Brandenburg, A. 2009, A&A, 495, 1
- Moffatt H. K. 1972, J. Fluid Mech., 53, 385
- Moffatt, H. K. 1978, Magnetic field generation in electrically conducting fluids (Cambridge University Press, Cambridge)
- Nordlund, Å., Brandenburg, A., Jennings, R. L., Rieutord, M., Ruokolainen, J., Stein, R. F., & Tuominen, I. 1992, ApJ, 392, 647
- Parker, E. N. 1979, Cosmical magnetic fields (Clarendon Press, Oxford)
- Pouquet, A., Frisch, U., & Léorat, J. 1976, J. Fluid Mech., 77, 321
- Rädler, K.-H., & Brandenburg, A. 2010, Astron. Nachr., 331, 14
- Rädler, K.-H., Rheinhardt, M. 2007, Geophys. Astrophys. Fluid Dyn., 101, 117
- Rädler, K.-H., Rheinhardt, M., Apstein, E., & Fuchs, H. 2002a, Magnetohydrodynamics, 38, 41
- Rädler, K.-H., Rheinhardt, M., Apstein, E., & Fuchs, H. 2002b, Nonl. Processes Geophys., 38, 171
- Rogachevskii I., Kleeorin N. 2000, Phys. Rev. E, 61, 5202
- Rogachevskii, I., & Kleeorin, N. 2007, Phys. Rev. E, 76, 056307
- Rüdiger G. 1974, Astron. Nachr., 295, 275
- Rüdiger, G. 1980, Geophys. Astrophys. Fluid Dyn., 16, 239
- Rüdiger, G. 1982, Geophys. Astrophys. Fluid Dyn., 21, 1
- Schekochihin, A. A., Maron, J. L., Cowley, S. C., & McWilliams, J. C. 2002, ApJ, 576, 806
- Schekochihin, A. A., Cowley, S. C., Taylor, S. F., Maron, J. L., & McWilliams, J. C. 2004, ApJ, 612, 276
- Schrinner, M., Rädler, K.-H., Schmitt, D., Rheinhardt, M., Christensen, U. 2005, Astron. Nachr., 326, 245
- Schrinner, M., Rädler, K.-H., Schmitt, D., Rheinhardt, M., Christensen, U. R. 2007, Geophys. Astrophys. Fluid Dyn., 101, 81
- Solanki, S. K., Inhester, B., & Schüssler, M. 2006, Rep. Prog. Phys., 69, 563

- Sulem, P. L., She, Z. S., Scholl, H., & Frisch, U. 1989, *J. Fluid Mech.*, 205, 341
- Sur, S., Subramanian, K., & Brandenburg, A. 2007, *MNRAS*, 376, 1238
- Sur, S., Brandenburg, A., & Subramanian, K. 2008, *MNRAS*, 385, L15
- Tilgner, A., & Brandenburg, A. 2008, *MNRAS*, 391, 1477
- Vögler, A., & Schüssler, M. 2007, *A&A*, 465, L43
- Yoshizawa, A. 1990, *Phys. Fluids B*, 2, 1589